https://doi.org/10.1016/j.buildenv.2023.110963

This is the Pre-Published Version.

Investigating the impact of gaspers on airborne disease transmission in an economy-class aircraft cabin with personalized displacement ventilation

Yunge Hou, Ruoyu You*

Department of Building Environment and Energy Engineering, The Hong Kong Polytechnic University, Kowloon, 999077, Hong Kong SAR, China

* Email: ruoyu.you@polyu.edu.hk

Abstract

Overhead gaspers provide directional fresh airflow, and thus affect the local airflow pattern and contaminant distribution. To investigate the impact of gaspers on airborne disease transmission in an aircraft cabin with a personalized displacement ventilation system, numerical calculations were conducted in a seven-row, single-aisle, fully occupied, economy-class aircraft cabin with the computational fluid dynamics (CFD) simulation method. We first investigated the impact of source gasper direction and flow rate on the airborne transmission near the contaminant source. We then investigated the protective effect of the receptor's gasper. For a source passenger's gasper, the direction and flow rate of the gasper flow either increased or decreased the air contaminant transmission to other passengers. Directing the source gasper to the abdomen with a medium flow rate performed best by reducing the receptors' mean exposure index by at least 45%, as this approach minimized the contaminant circulation in the cabin. Turning on a receptor passenger's gasper could be an effective strategy to protect the receptor, and the working mechanism was revealed. The gasper-induced jet flow entrained the surrounding air into the jet region, and the protective effect was related to the contaminant concentration at ceiling level. With a suitable gasper direction and flow rate, the gasper jet formed a virtual barrier between the source passenger and the receptor. When the contaminants were transported upwards to a receptor's breathing zone, turning on the receptor's gasper reduced the contaminant concentration, since the downward gasper jet altered the airflow pattern in front of the receptor.

Keywords

Airborne disease transmission; Gasper; Personalized displacement ventilation; Computational fluid dynamics; Exposure index

© 2023. This manuscript version is made available under the CC-BY-NC-ND 4.0 license http://creativecommons.org/licenses/by-nc-nd/4.0/

1. Introduction

According to the International Air Transport Association (IATA), more than 3.7 billion passengers travelled by air in 2022, an increase of 73% over 2021 [1]. The rapidly growing number of air passengers increases the risk of airborne disease transmission in aircraft cabins because of the high occupant density and long exposure time, as has been widely reported [2-6]. The air distribution system plays a major role in controlling air quality in aircraft cabins [7-10]. Therefore, it is crucial to investigate the impact of air distribution systems on airborne disease transmission in aircraft cabins for the health of the general public.

Mixing ventilation systems are commonly utilized in commercial airliners to provide a suitable cabin environment. A mixing ventilation system supplies fresh air to the cabin at ceiling and/or shoulder level and removes the cabin air through the side walls at floor level. However, mixing ventilation is not efficient in controlling contaminant transport [11-14]. Displacement ventilation systems have been found more effective than mixing ventilation systems in removing contaminants and improving cabin air quality [15]. The reason is that the displacement ventilation system supplies fresh air at floor level and removes the cabin air at ceiling level; thus, the airflow pattern is consistent with the thermal plumes created by passengers. In addition, personalized ventilation systems have been developed to effectively reduce the infection risk in cabins by supplying fresh air directly to the breathing zone of the passengers [8, 16-19]. For instance, You et al. [19] proposed an innovative personalized displacement ventilation system with individual diffusers installed on the floor under the seats. Clean air was supplied directly to the passengers in the row behind, and then exhausted at ceiling level. They found that the personalized system reduced the average exposure in the cabin by more than 50% compared with traditional mixing and displacement ventilation systems [13, 19].

In addition to the main ventilation system, a system of gaspers is also available in most commercial airliners for individual ventilation and thermal regulation. Gaspers are a system of small, circular, adjustable vents installed above the seat for each passenger. Previous studies have indicated that gasper jets alter the air distribution and thus have a substantial impact on contaminant transport in the cabin [20-26]. For example, Dai et al. [20] used a high precision hot-wire anemometer to collect velocity and turbulence intensity data in the flow field of gasper isothermal jet. They found that the flow field was complicated near the nozzle but could be simplified as a round jet when fully developed. Shi et al. [21] employed computational fluid dynamics (CFD) to simulate gasper-induced jet flow, and found that when the gasper jet was discharged, the disturbances developed into vortices, forming coherent structures. These coherent structures grew continuously as they were transported downstream, greatly enhancing the mixing process between the gasper-induced jet and the ambient fluid. Li et al. [22] used a Particle Image Velocimetry (PIV) system to investigate the interactions between gasper jets and the main ventilation. They found that the gasper significantly increased the air velocity in target passenger's

breathing zone. However, opening the gasper with medium or high flow rate decreased the air velocity around the adjacent passenger. As for the impact of gaspers on air quality, Li et al. [23] measured the distributions of air velocity, temperature, and contaminant concentrations in an MD-82 cabin with two of five gaspers on. Although the gaspers directed clean air toward the passengers, the air quality in the breathing zone was not improved in this case. You et al. [24-26] statistically investigated the impact of gasper-induced jet flow on receptors' exposure to contaminants exhaled by an index passenger in cabins with mixing ventilation. According to their results, although the gaspers' on/off distribution significantly influenced the infection risk for each passenger, the overall effect of turning on a passenger's gasper on the mean infection risk for the passengers was not conclusive. In other words, turning on a passenger's gasper could result in either a positive or negative impact on his/her infection risk.

Although the above studies have provided great insight into gasper-induced jet flow and its influence on air quality, there is a lack of systematic studies of the impact of gasper settings on airborne disease transmission in cabins, as passengers usually adjust the direction and flow rate of gaspers to help achieve their preferred cabin environment [27-29]. Moreover, Li et al. [23] reported that the contaminant was pushed down to the lower part of the cabin when the gaspers were on. This indicates that turning on gaspers may increase the exposure risk for other passengers, especially in a cabin with a personalized displacement ventilation system. The reason is that gasper-induced jet flow is directed downwards, while the main flow and thermal plume generated by passengers travel upwards. However, the interaction of the flows from different directions and the impact of this interaction on contaminant transport have not been well explored. Therefore, further efforts should be made to systematically investigate the impact of gaspers on airborne disease transmission in aircraft cabins with personalized displacement ventilation.

To investigate air distributions in cabins, the experimental measurements were more reliable but expensive and time consuming, while CFD simulation could effectively provide more detailed information [30]. Considerable efforts has been made to seek more reliable and accurate turbulence models, especially for complex flows [24, 26, 31]. For instant, Shi et al [31] systematically evaluated the performances of most prevalent models in simulating stratified flows, including six Reynolds-averaged Navier–Stokes models and one large eddy simulation model. They found that the shear stress transport (SST) k–ω model was the best for the strongly stratified jet. You et al. [24] used measured data to evaluate the performance of the re-normalization group (RNG) k–ε model and the SST k–ω model for predicting air distribution in cabins with gasper on, and the SST k–ω model was found to be more accurate in gasper-induced jet dominant region. Therefore, CFD is a reliable tool for modelling gasper-induced jet flow in aircraft cabins.

To fill the research gap and provide a reference for gasper settings from the perspective of public health, the present study first investigated the impact of source gasper direction and flow rate on airborne disease transmission near the source in a seven-row, single-aisle, fully occupied, economy-class aircraft cabin with the CFD method. Next, we evaluated the protective effect of the receptor's gasper. Finally, we identified the most effective gasper settings for source passengers and the working mechanism of the receptor's gasper.

2. Methodology for airflow simulation

The CFD method was adopted in this study for calculating air distribution and airborne disease transmission, and ANSYS Fluent was used [32]. The SST *k*-*ω* model [33] was used for predicting the steady-state air distribution in aircraft cabins with gaspers on, considering that this model performs best for a jet flow [21, 24, 25, 31]. In the SST *k*-*ω* model, the turbulence kinetic energy (k) and the specific dissipation rate (ω) are obtained from the following transport equations [32]:

$$\frac{\partial}{\partial t}(\rho k) + \frac{\partial}{\partial x_i}(\rho k U_i) = \frac{\partial}{\partial x_j}\left[\left(\mu + \frac{\mu_t}{\sigma_k}\right)\frac{\partial k}{\partial x_j}\right] + G_k - Y_k \quad (1)$$

$$\frac{\partial}{\partial t}(\rho \omega) + \frac{\partial}{\partial x_i}(\rho \omega U_i) = \frac{\partial}{\partial x_j}\left[\left(\mu + \frac{\mu_t}{\sigma_\omega}\right)\frac{\partial \omega}{\partial x_j}\right] + G_\omega - Y_\omega + D_\omega \quad (2)$$

where σ_k and σ_ω are the turbulent Prandtl number for k and ω, respectively. Meanwhile, G_k represents the generation of k due to mean velocity gradients; G_ω represents the generation of ω; Y_k and Y_ω represent the dissipation of k and ω, respectively, due to turbulence; and D_ω is the cross-diffusion term.

The Eulerian method [34] was used to simulate contaminant transport in aircraft cabins, as this method has been widely used in previous studies on airborne disease transmission [35-38]:

$$\frac{\partial \rho \phi}{\partial t} + \frac{\partial}{\partial x_i}\left(\rho \phi U_i - \Gamma_\phi \frac{\partial \phi}{\partial x_i}\right) = S_\phi \quad (3)$$

where ϕ is contaminant concentration, t is time, ρ is density, U_i is air velocity, Γ_ϕ is the diffusion coefficient, and S_ϕ is the mass flow rate of contaminant source per unit volume. This study used User-Defined Scalar (UDS) to simulate the contaminant, and a scalar transport equation was activated in ANSYS Fluent.

In this study, the Boussinesq approximation was adopted to consider the buoyancy effect [39]. The SIMPLE algorithm [40] was employed for coupling pressure-velocity equations. The PRESTO! scheme was used for discretizing pressure, and the second-order scheme was used for all the other variables. This investigation assumed that the calculation reached convergence with velocity residuals at 10^{-4}, turbulence residuals at 10^{-5}, and the energy residual at 10^{-6}.

Note that there is no experimental airflow data available in the literature for the interaction between displacement ventilation, gasper-induced jet flow, and thermal plume. As this study aimed to investigate the impact of gasper-induced flow on the contaminant transport, experimental data from You et al. [24] was used to validate the airflow simulation. The experimental measurements were conducted in a half-row, single-aisle aircraft cabin mock-up with mixing ventilation, as shown in Fig. 1(a), with dimensions of 1.75 m in width (x), 0.9 m in depth (y), and 2.2 m in height (z). The main airflow was provided by a linear diffuser on the aisle ceiling with a velocity of 1.44 m/s. Additional air was supplied through a gasper installed on the inclined ceiling at a flow rate of 1.2 L/s. The air was exhausted at floor level. The total flow rate of the cabin mock-up was 27.1 L/s, corresponding to an air change rate of 33.5 ACH. A heated box was placed inside the cabin with a heat load of 75 W to represent a passenger. A PIV system was used to obtain the airflow in the measuring area, as shown in Fig. 1(b). The velocity profiles along three lines were compared with the simulation results for validation. For further details, readers may refer to the original experimental work [24].

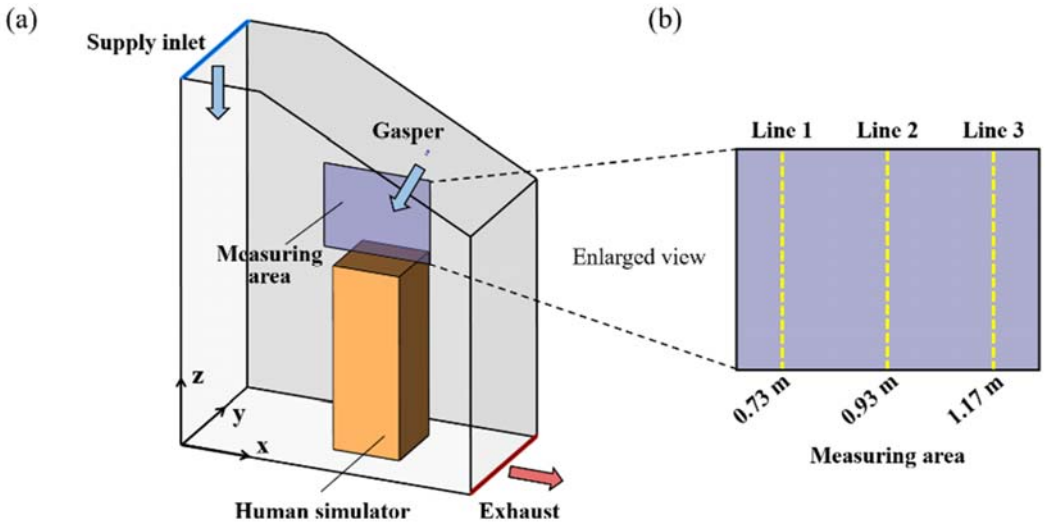

Fig. 1. Sketch of (a) the aircraft cabin mock-up with a gasper on (revised from [24]), and (b) the measuring area.

The comparison of the simulated horizontal velocity component and vertical velocity component with the experimental data along Lines 1-3 are shown in Fig. 2. The simulated velocity component profiles agreed well with the measured data. Therefore, the complex interaction of the main flow, gasper-induced jet flow, and thermal plume can be accurately predicted.

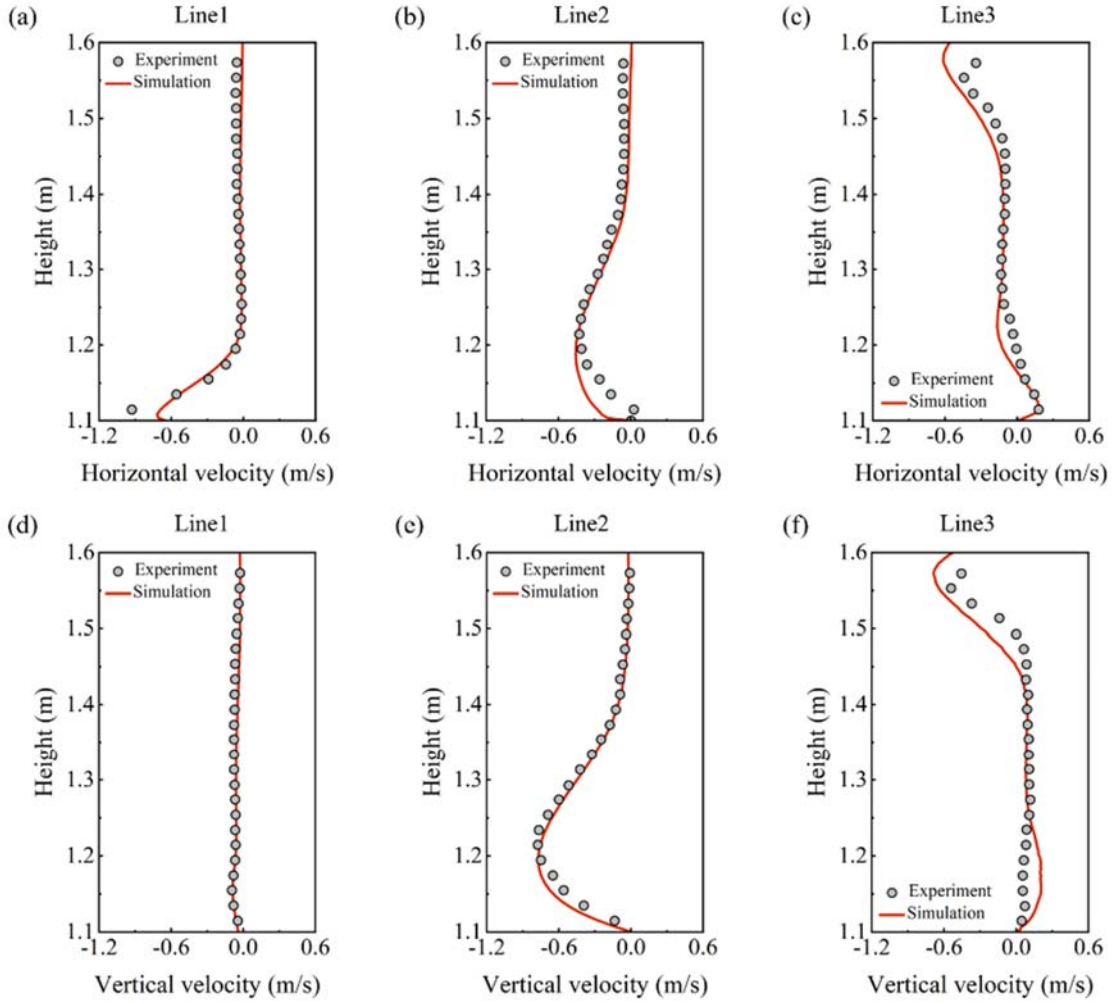

Fig. 2. Comparison of the simulated and measured (a-c) horizontal velocity component and (d-f) vertical velocity component along Lines 1-3.

3. Case setup

A seven-row, single-aisle, fully occupied, economy-class aircraft cabin with a personalized displacement ventilation system is illustrated in Fig. 3(a). In this system, 42 individual diffusers (300 mm in height and 80 mm in width) were installed, one diffuser under each seat, to provide clean air directed towards the breathing zone of the passengers in the row behind the seats. A system of gaspers was installed on the ceiling. The total flow rate of supply air was 320.46 L/s [19], corresponding to an air change rate of 39.7 ACH. The cabin air was exhausted through two slots with a width of 4 mm at the ceiling center. The turbulence intensity at the diffusers and gaspers was assumed to be 10%, and the turbulence length scale was set as the opening width [13]. The temperature of the supply air was 19.3 ℃ [13]. The surface temperatures of the floor, sidewalls, ceiling, and passengers were 23.8 ℃, 24.5 ℃, 25.0 ℃, and 31.0 ℃, respectively [13]. In some aircraft types such as Boeing 737 or Airbus A320, a separate class is outfitted with 25 rows of seats [41]. Therefore, a 25-row section model with wall

boundaries for the front and rear surfaces closely resembles a real-life scenario. Accordingly, we also simulated the air distribution in a 25-row section of an aircraft cabin to provide momentum and thermal data for the front and rear surfaces of the seven-row section model. The breathing flow rate caused by constantly exhaling or constantly inhaling was not considered in this study. Contaminants were released continuously with zero momentum from a cube (100 mm in side length) in front of the mouth of the source passenger. For a specific receptor, we used the exposure index [42] to quantify the relative intake of contaminants exhaled by the source passenger, as this index has been widely adopted in previous studies [19, 43-45]. The exposure index ε was defined as the ratio of the contaminant concentration in a receptor's breathing zone to the contaminant concentration in the return air [42]. The breathing zone was assumed to be a hemisphere in front of the shoulders, centered on the mouth and nose, with a radius of 20 cm [46], as shown in Fig. 3(b).

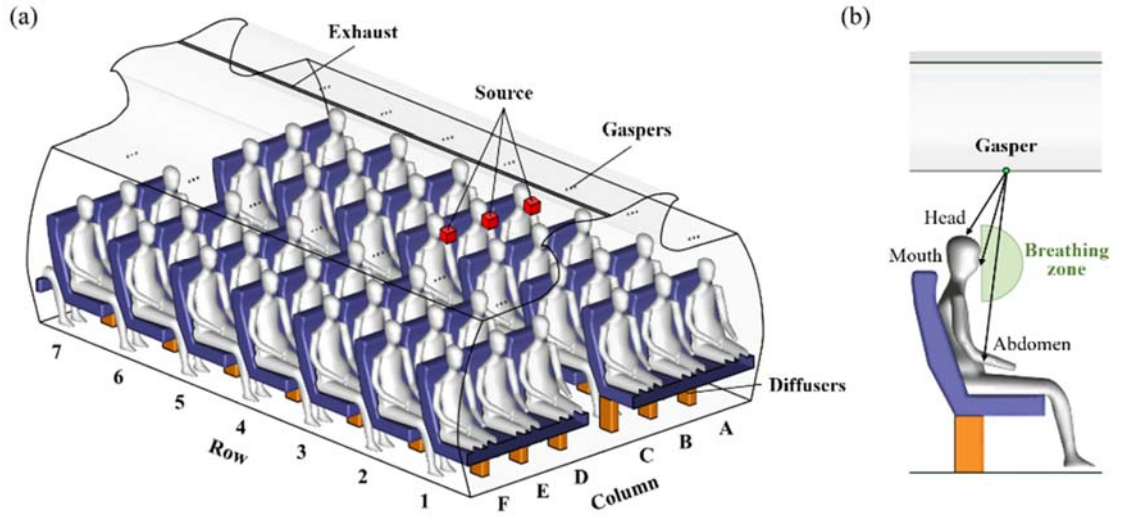

Fig. 3. (a) Schematic of a seven-row section of the single-aisle, fully occupied, economy-class aircraft cabin and (b) the breathing zone and gasper directions in the side view.

To investigate the impact of gaspers on near-source transmission, we considered three source locations according to symmetry: the source passenger seated at 4A (window seat), 4B (middle seat), and 4C (aisle seat). The other passengers' gaspers were assumed to be closed. For the source passenger's gasper, the flow rates of 0.66 L/s (half-open) [23] and 1.32 L/s (fully open) were considered, and turning the gasper off was used as a benchmark. In a previous study, Fang et al. [27] experimentally found that more than 68% of participants adjusted the gaspers to target their bodies above waist level. Therefore, in the present study, three directions were considered (see Fig. 3(b)) for the source passenger's gasper direction: to the head (H), to the mouth (M), and to the abdomen (A). A total of 21 cases were calculated. To investigate the impact of the receptor's gasper, we focused on the three most at-risk receptors with the highest exposure for each seat type, and the gaspers of other receptors were assumed to be closed. Another 18 cases were calculated, and the total number of cases in this study was 39.

A grid-independence test was conducted in a one-row section of the cabin with three grid resolutions, a coarse grid of 0.48 million, a moderate grid of 1.20 million, and a fine grid of 3.24 million. As shown in Fig. 4(a), we compared the air velocity along the vertical centerline of the aisle (Line 1) and the gasper-induced jet flow direction (Line 2). The results in Fig. 4(b)-(c) clearly showed that the moderate grid was adequate to capture the main flow and jet flow in the cabin.

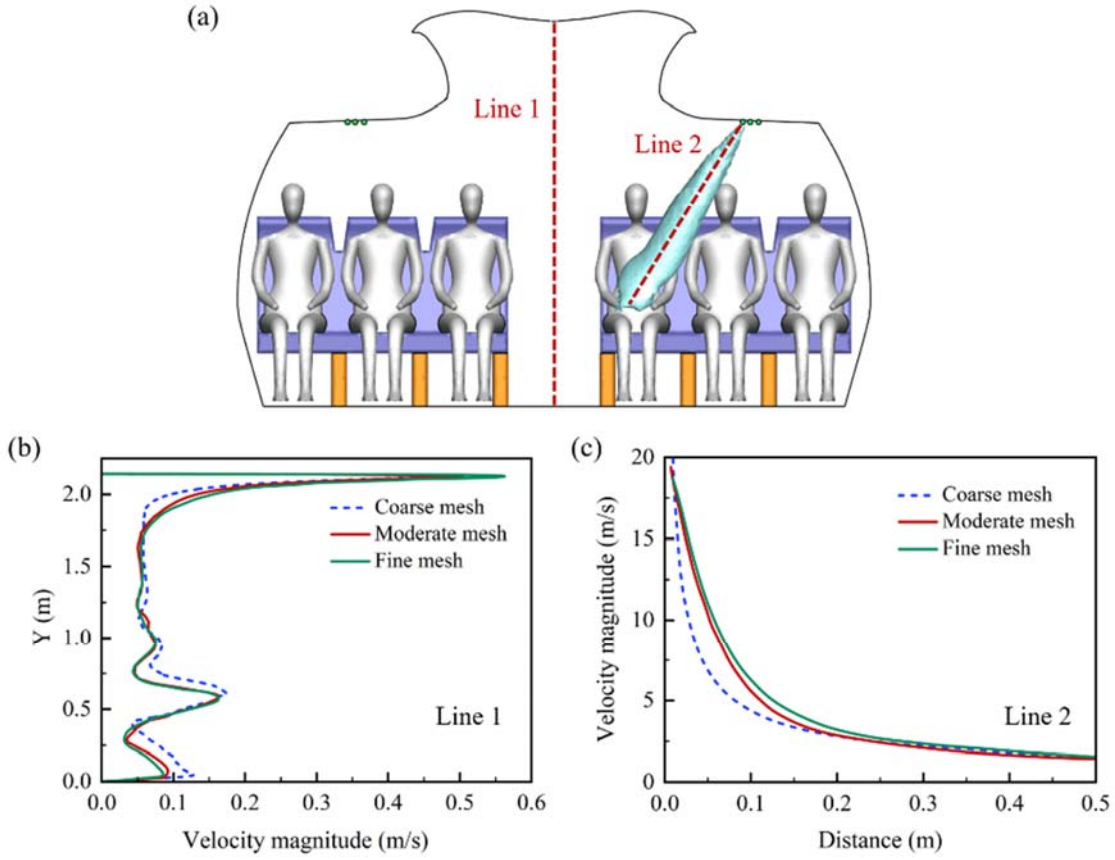

Fig. 4. (a) The one-row section of aircraft cabin for grid independence test, and comparison of the velocity profiles at (b) Line 1 and (c) Line 2.

With the above moderate grid resolution, the grid distribution employed in this study is shown in Fig. 5. The smallest meshes used around the exhaust and gaspers were 1 mm (labeled as ①) and 1.4 mm (labeled as ②), respectively. The size of the mesh on the passenger surfaces was 25 mm to depict the complex geometry. In other areas, the mesh size increased gradually by a factor of 1.2 to a maximum size of 60 mm. This led to a total grid number of 8.36 million for the seven-row section model.

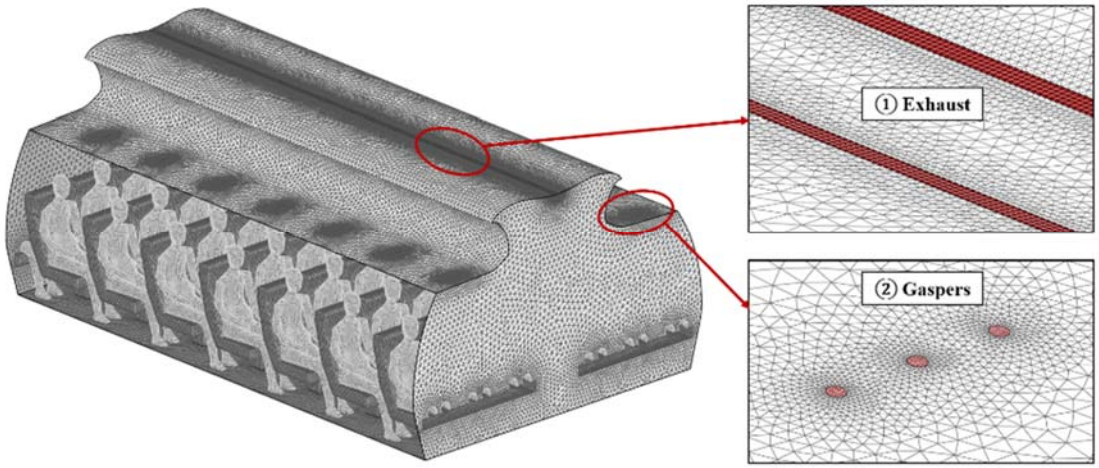

Fig. 5. Grid distribution for the seven-row section of aircraft cabin.

4. Impact of source gasper on near-source transmission

To investigate the impact of gaspers on near-source transmission, we first analysed the airflow pattern and exposure index of the receptors when the source passenger was in different seat locations with all gaspers off as the benchmark. We then compared the exposure index under different source gasper settings, including directions and flow rates. Finally, we assessed the performance of different gasper settings in reducing overall exposure to obtain the optimal gasper setting for source passengers.

4.1 Gaspers off

When all gaspers were turned off, the air distribution in the cabin was dominated by the main flow and thermal plume. The airflow pattern in the cross section located 0.05 m in front of the mouth of the passengers in the fourth row (CS4) is shown in Fig. 6(a). The red arrows represent the general airflow structure. At breathing level, the air at the window seat moved towards the sidewall, while the air at the aisle seat moved towards the aisle. The air at the middle seat moved upwards due to the thermal plume. At ceiling level, the air ascended to the exhaust in the ceiling center. In the lower part of the aisle, the air descended to the floor and then moved to the region under the seats on both sides. The airflow pattern in the horizontal section at breathing level (HS) is shown in Fig. 6(b). It can be seen that the airflow at breathing level was forward.

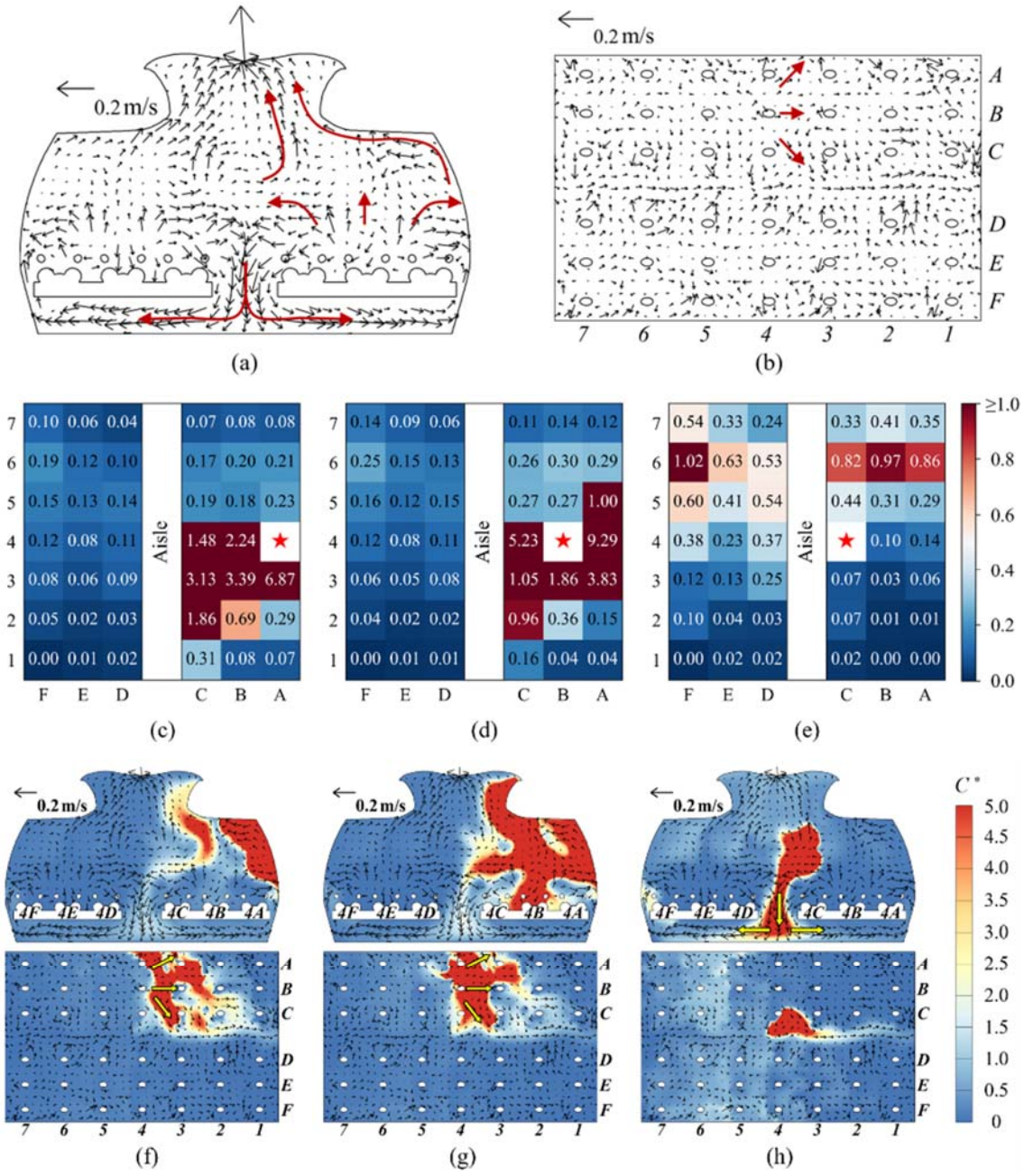

Fig. 6. The airflow patterns at (a) CS4 and (b) HS, (c-e) the exposure index, and (f-h) the *C** distributions at CS4 and HS with source passenger in the window seat, middle seat, and aisle seat.

The exposure index of the receptors with source passenger in different seat locations are shown in Fig. 6(c)-(e). The red star represents the source location. When the source passenger was in the window or middle seat (see Fig. 6(c) and (d)), passengers with higher exposure index were clustered in the few rows directly in front of the source passenger. However, when the source passenger was in the aisle seat (see Fig. 6(e)), passengers behind the source passenger had higher exposure risk.

To analyse the contaminant transmission route, we also compared the dimensionless contaminant concentration C^* (normalized by the contaminant concentration of return air) distributions at CS4 and HS with different source locations, as shown in Fig. 6(f)-(h). When the source passenger was in the window or middle seat, the contaminants moved forward due to the forward airflow at breathing level (see Fig. 6(f) and (g)). When the source passenger was in the aisle seat, a considerable amount of the exhaled contaminants was transported downwards to the aisle floor (see Fig 6(h)), moved to both sides, and finally entered the breathing zone of the passengers in the back rows. Therefore, the passengers behind the source passenger were exposed to a higher concentration of contaminants.

4.2 Source gasper on

The relative positions of the source passenger and his/her gasper were different for each source location, as shown in Fig. 7. The green arrows represent the general direction of the gasper-induced jet flow. When the source passenger was seated in the window seat, the source gasper was in front of the right side of the source passenger, and the gasper flow thus moved backwards and left towards the sidewall. In contrast, when the source passenger was seated in the middle or aisle seat, the gasper of the source passenger was in front of the left side of the source passenger. Therefore, the gasper flow moved backwards and right towards the aisle.

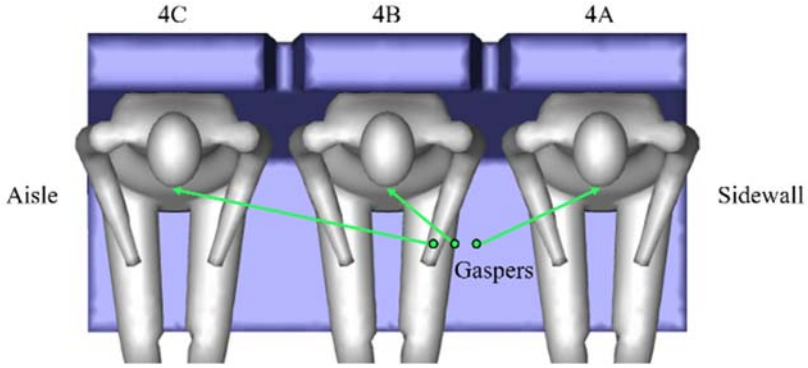

Fig. 7. Relative positions of source passengers and gaspers in the top view.

4.2.1 Window seat

When the source passenger was in the window seat 4A, three directions (see Fig. 3(b)) and two flow rates of the source gasper were considered. We compared the exposure index under different source gasper settings, as shown in Fig. 8(a)-(c). To keep the paper concise, only the results for some of the cases are presented, and the remaining results can be found in Appendix. The results show that opening the source gasper increased the exposure index of receptors behind the source passenger, particularly when the flow rate was high. For instance, when the source gasper was fully open towards the mouth (see Fig. 8(b)), the exposure index of five of the receptors behind the source passenger was above 1, in contrast with the benchmark case, where the exposure index of all receptors behind the source passenger was less than 1 (see Fig. 6(c)).

To clarify the influence mechanism of the gasper, we further analysed the airflow pattern and C^* distribution at CS4, HS, and the longitudinal section for passengers in column A (LSA), as shown in Fig. 8(d)-(f). When the source gasper was open, as the gasper-induced flow was towards the sidewall (see Fig. 7), the jet flow entrained the contaminants backwards to the sidewall. With a higher flow rate, the gasper jet flow gained more momentum and transported the contaminants further towards the rear rows. Simultaneously, a portion of the contaminants was transported to the floor and then entered the breathing zone of rear receptors by upwards flow from the diffusers, as shown in Fig. 8(e). However, when the gasper was half-open to the abdomen, the jet flow was blocked by the body of the source passenger, as depicted in Fig. 8(f), preventing the backward transmission of contaminants. Therefore, the exposure index of rear receptors was not notably increased (see Fig. 8(c)).

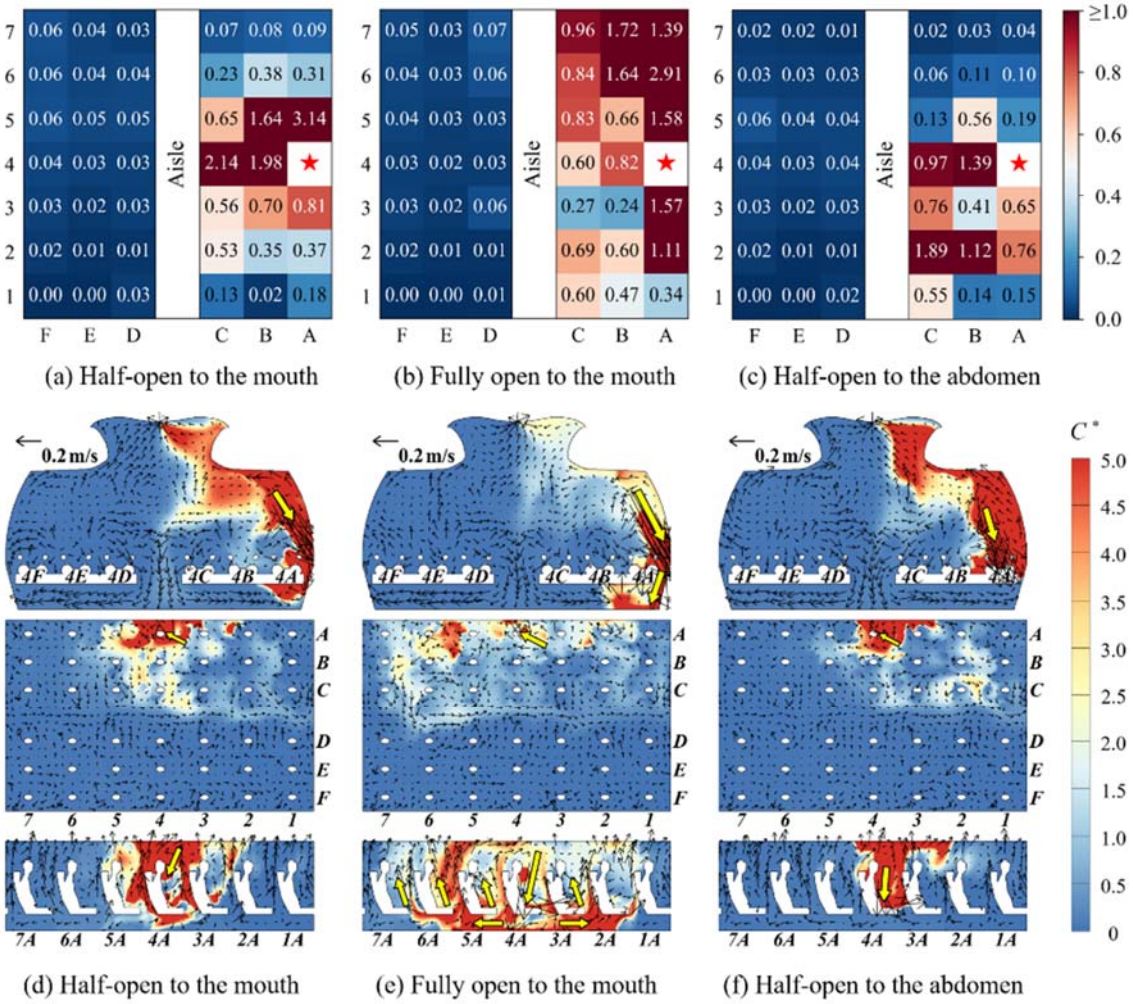

Fig. 8. (a-c) Exposure index, and (d-f) the airflow patterns and C^* distributions at CS4, HS, and LSA under different gasper settings with source passenger seated in the window seat 4A.

4.2.2 Middle seat

When the source passenger was in the middle seat 4B, three directions (see Fig. 3(b)) and two flow rates of the source gasper were considered. The exposure index under different source gasper settings are shown in Fig. 9(a)-(c). The results indicate that when the source gasper was open, the exposure index of receptors behind the source passenger even on the opposite side of the aisle was increased, while the exposure index of receptors in front of the source passenger was decreased. To explain this phenomenon, we analysed the airflow patterns and C^* distributions at CS4, HS, and the longitudinal section for passengers in column B (LSB), as shown in Fig. 9(d)-(f). When the source gasper was open, as the gasper-induced flow was towards the aisle, the jet flow entrained the contaminants backwards to the aisle (see Fig. 7). If the gasper was open at a high flow rate, the gasper-induced flow gained more momentum, and entrained the contaminants further backwards even across the aisle (Fig. 9(e)). However, with a lower flow rate, the momentum of gasper-induced flow was insufficient to transport the contaminants across the aisle (see Fig. 9(d) and (f)). Instead, the contaminants were transported to the aisle, carried by the main flow to the aisle floor, and finally moved to the receptors in the rear rows.

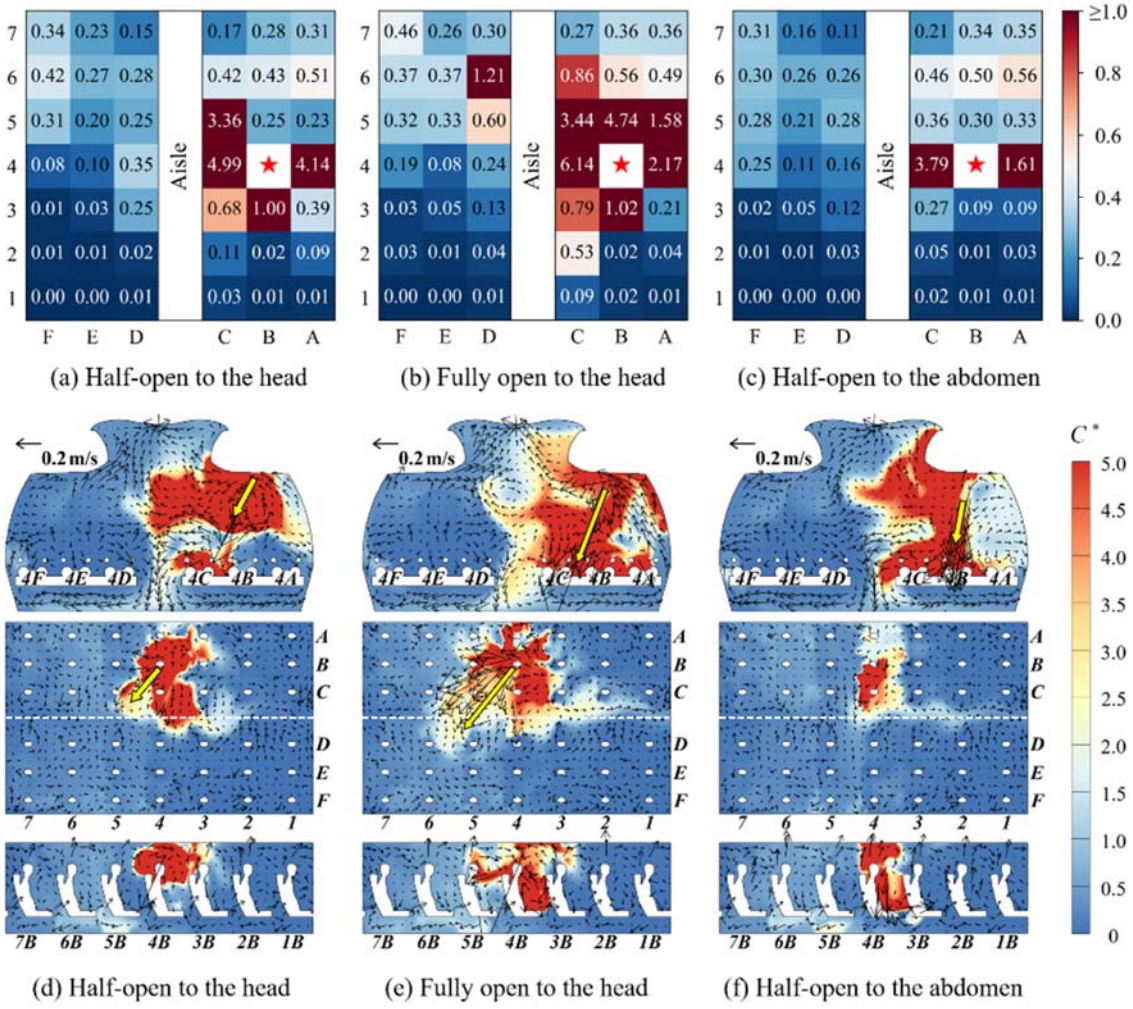

Fig. 9. (a-c) Exposure index, and (d-f) the airflow patterns and C^* distributions at CS4, HS, and LSB under different gasper settings with source passenger seated in the middle seat 4B.

4.2.3 Aisle seat

When the source passenger was in the aisle seat 4C, three directions (see Fig. 3(b)) and two flow rates of the source gasper were considered. We compared the exposure index under different source gasper settings, as shown in Fig. 10(a)-(c). It can be seen that when the source gasper was half-open to the abdomen, the exposure index of almost all receptors was reduced (see Fig. 10(b)). As for other source gasper settings, the exposure of receptors behind the source passenger even on the opposite side of the aisle was increased, while the exposure of receptors in front of the source passengers was decreased, which was similar to the situation when the source passenger was in the middle seat with the gasper on.

Next, we analysed the airflow pattern and C^* distribution at CS4, HS, and the longitudinal section for passengers in column C (LSC), as shown in Fig. 10(d)-(f). The results indicate that the airborne transmission routes varied under different source gasper settings. For example, when the source gasper was half-open to the head, as illustrated in Fig. 10(d), some of the exhaled contaminants were entrained by the gasper-induced jet flow and directly entered the breathing zone of the receptors on the opposite of the aisle. Meanwhile, the other portion of contaminants were transported downwards to the aisle floor and then entered the breathing zone of the receptors in the rear rows. When the source gasper was fully open to the abdomen, as shown in Fig. 10(f), the gasper-induced flow entrained a considerable amount of the exhaled contaminants across the aisle to the floor. The contaminants were then transported to the breathing zone of the receptors in the rear rows. However, when the source gasper was half-open to the abdomen, the contaminants were not transported across the aisle due to obstruction by the body of the source passenger. Instead, the contaminants were carried by the main flow and then exhausted directly through the ceiling center, as shown in Fig. 10(e).

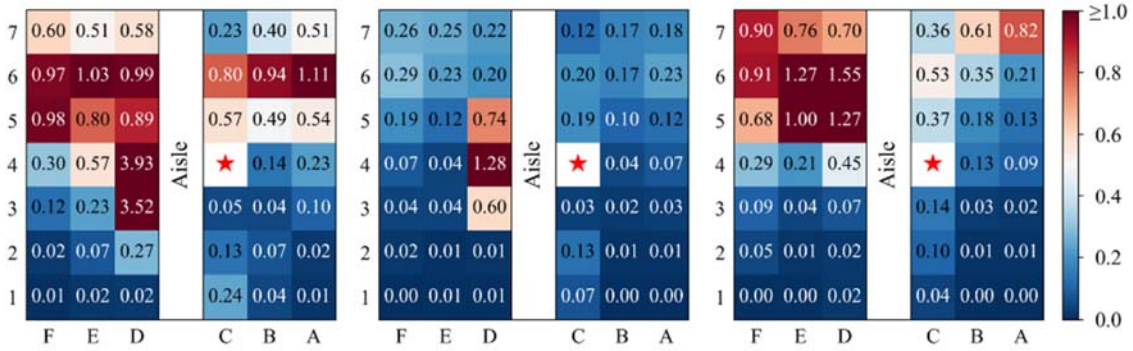

(a) Half-open to the head (b) Half-open to the abdomen (c) Fully open to the abdomen

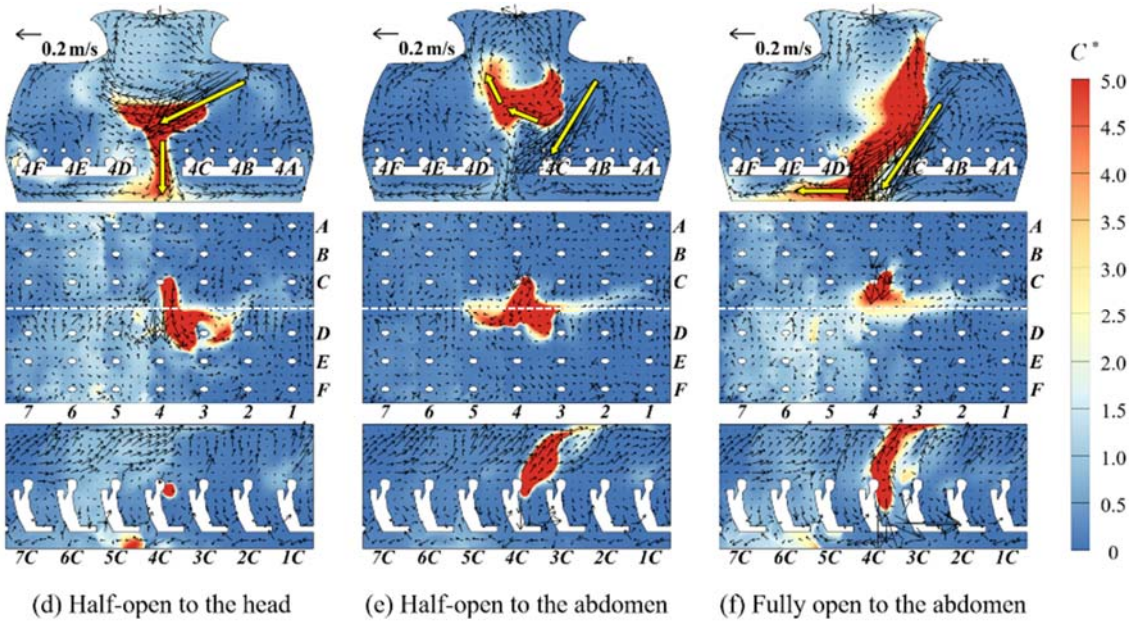

Fig. 10. (a-c) Exposure index, and (d-f) the airflow patterns and C^* distributions at CS4, HS, and LSC under different gasper settings with source passenger seated in the aisle seat 4C.

4.3 Assessment of different source gasper settings

For a quantitative assessment of the performance of different source gasper settings, Table 1 displays the mean exposure index of all receptors (ε_{mean}) and the number of receptors with an exposure index above 1 ($No_{\varepsilon>1}$) for different source gasper settings with different source locations. It can be seen that the source passenger's setting could result in either a positive or negative impact on the mean exposure index of all receptors. Taking the source passenger seated at 4C as an example, when the source gasper was half-open to the abdomen, the mean exposure of all receptors was 0.16, which was 45% lower than the benchmark (0.29). In contrast, when the source gasper was half-open to the head, the mean exposure was 0.56, almost twice the benchmark level.

Table 1. ε_{mean} and $No_{\varepsilon>1}$ for different gasper settings with different source locations.

Source location	Assessment indicator	Gasper off	Head half-open	Head fully open	Mouth half-open	Mouth fully open	Abdomen half-open	Abdomen fully open
4A	ε_{mean}	0.57	0.32	0.58	0.37	0.50	0.26	0.27
	$No_{\varepsilon>1}$	6	4	10	4	7	3	4
4B	ε_{mean}	0.67	0.51	0.70	0.53	0.54	0.30	0.48
	$No_{\varepsilon>1}$	5	3	7	2	3	2	4
4C	ε_{mean}	0.29	0.56	0.55	0.39	0.48	0.16	0.35
	$No_{\varepsilon>1}$	1	4	10	5	6	1	3

The number of receptors with an exposure index above 1 should also be considered in addition to the mean exposure. Taking the source passenger seated at 4A as an example, when the source gasper was fully open to the mouth, although the mean exposure (0.50) was lower than the benchmark (0.57), the value of $No_{\varepsilon>1}$ (7) was higher than the benchmark (6). Thus, more receptors were exposed to high infection risk when the source gasper was fully open to the mouth.

Among all gasper settings for each source location, keeping the gasper half-open towards the abdomen resulted in the lowest ε_{mean} and $No_{\varepsilon>1}$, and it reduced the ε_{mean} by at least 45%. This is because more contaminants were exhausted directly through the ceiling center, and the contaminant circulation in the cabin was reduced. Therefore, keeping the gasper half-open to the abdomen is recommended for source passengers.

5 Impact of receptor's gasper

To evaluate the effectiveness of gaspers in protecting receptors, we first identified the most at-risk receptor for each seat location as the target receptors. We then compared the exposure index of a given target receptor under different receptor gasper directions and flow rates to quantify the impact of the receptor's gasper settings. Furthermore, we analysed the airflow pattern and C^* distribution to characterize the working mechanism of the gasper.

5.1 Window seat

According to the exposure index in Section 4, the highest exposure index among all receptors in the window seat was 9.29 (see Fig. 6(d)). This receptor was seated at 4A, with the source passenger in 4B keeping the source gasper off, as shown in Fig. 11(a). We considered different directions and flow rates of the receptor's gasper, and the calculated exposure index of the receptor 4A is shown in Fig. 11(b). Turning the receptor's gasper off was used as the benchmark, with an exposure index of 9.29. When the receptor's gasper was directed to the head or mouth, keeping the gasper fully open performed better, whereas a half-open gasper was worse than the benchmark. For example, when the receptor's gasper was half-open to the head, the receptor's exposure index was 25.40, almost three times the benchmark. In contrast, the exposure index was only 2.74 when the gasper was fully open to the head, 71% lower than the benchmark. Possible reasons are as follows. In the benchmark case, as shown in Fig 11(c), the air at source passenger 4B moved leftwards, rightwards, and upwards, resulting in high contaminant concentration at 4A, 4C, and ceiling level. When the receptor's gasper was open, the jet flow from the ceiling entrained the contaminants into the receptor's breathing zone, as shown in Fig. 11(d), resulting in higher contaminant concentration compared with the benchmark. With a high flow rate, the entrained contaminants were quickly carried away to the sidewall and the back row, as shown in Fig. 11(e).

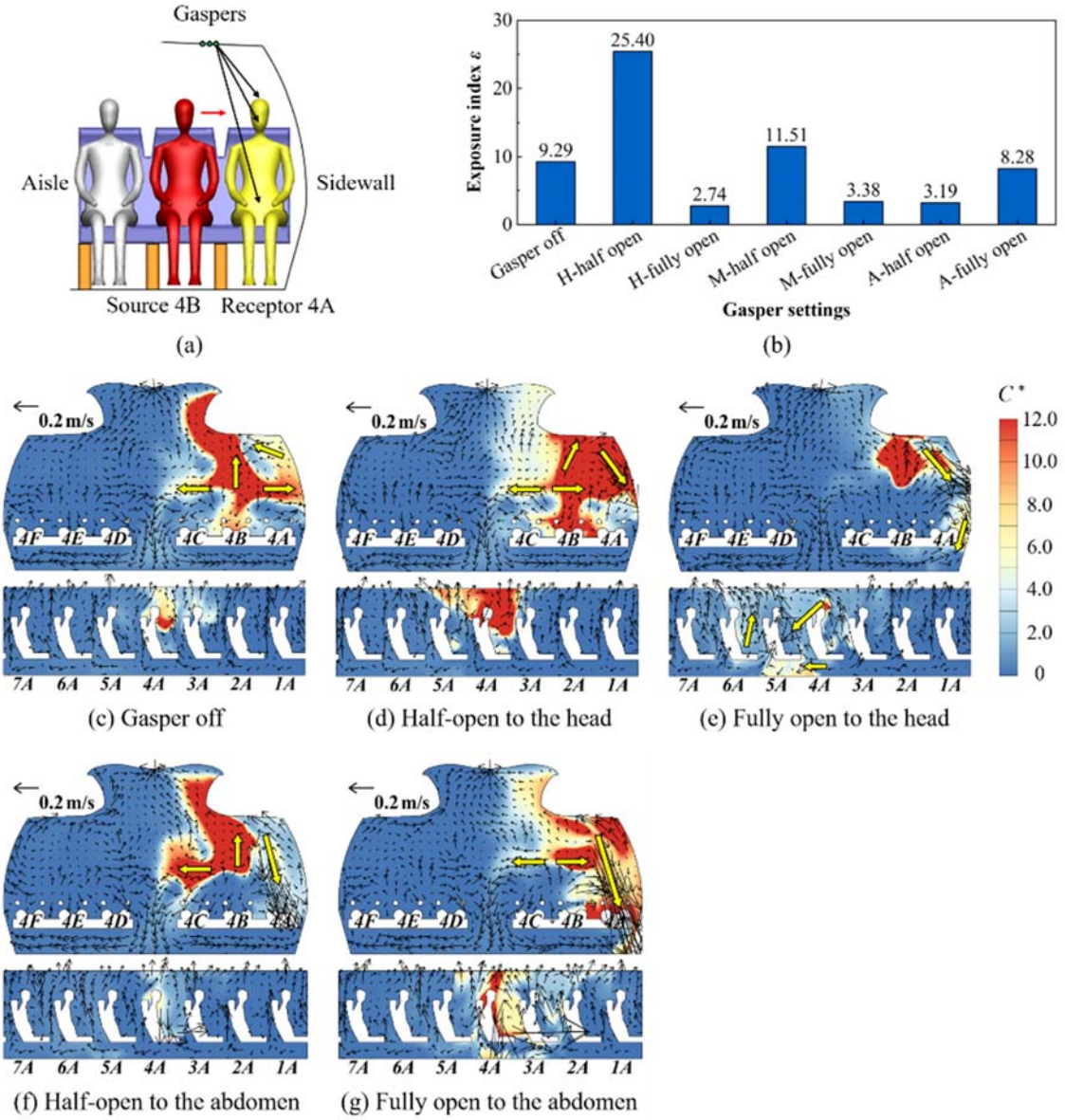

Fig. 11. (a) The relative positions of the source passenger and the receptor, (b) exposure index of the receptor 4A, and (c-g) airflow patterns and C^* distribution at CS4 and LSA under different receptor gasper settings.

Additionally, when the receptor's gasper was directed to the abdomen, opening the gasper with a medium flow rate performed much better than the benchmark. As shown in Fig. 11(a), the gasper jet when directed to the abdomen was positioned between the source passenger and the receptor. When the gasper was half-open as in Fig. 11(f), the gasper jet formed a virtual barrier between the source passenger and the receptor and thus reduced the contaminant concentration in the receptor's breathing zone [47]. However, with a high flow rate, as shown in Fig. 11(g), the gasper jet from the ceiling entrained the contaminants at ceiling level, resulting in a higher contaminant concentration in the receptor's breathing zone compared with the low flow rate scenario.

5.2 Middle seat

Among all receptors in the middle seats, the highest exposure index was 4.74 (see Fig. 9(b)). This most at-risk receptor was seated at 5B, with the source passenger in 4B keeping the source gasper fully open to the head, as shown in Fig. 12(a). The exposure index of the receptor 5B under different gasper settings is shown in Fig. 12(b). The results indicate that opening the receptor's gasper performed better than the benchmark. The exposure index of the receptor 5B with the gasper turned on ranged from 2.19 to 3.93, all lower than the benchmark. In the benchmark case, the contaminants were transported backwards at breathing level from the source passenger to the receptor, as indicated by the yellow arrow in Fig. 12(c), and the contaminant concentration at ceiling level above 5B was low. When the receptor's gasper was open, the jet flow from the ceiling entrained the clean air into the receptor's breathing zone, as shown in Fig. 12(d) and (e), resulting in a lower contaminant concentration compared with the benchmark.

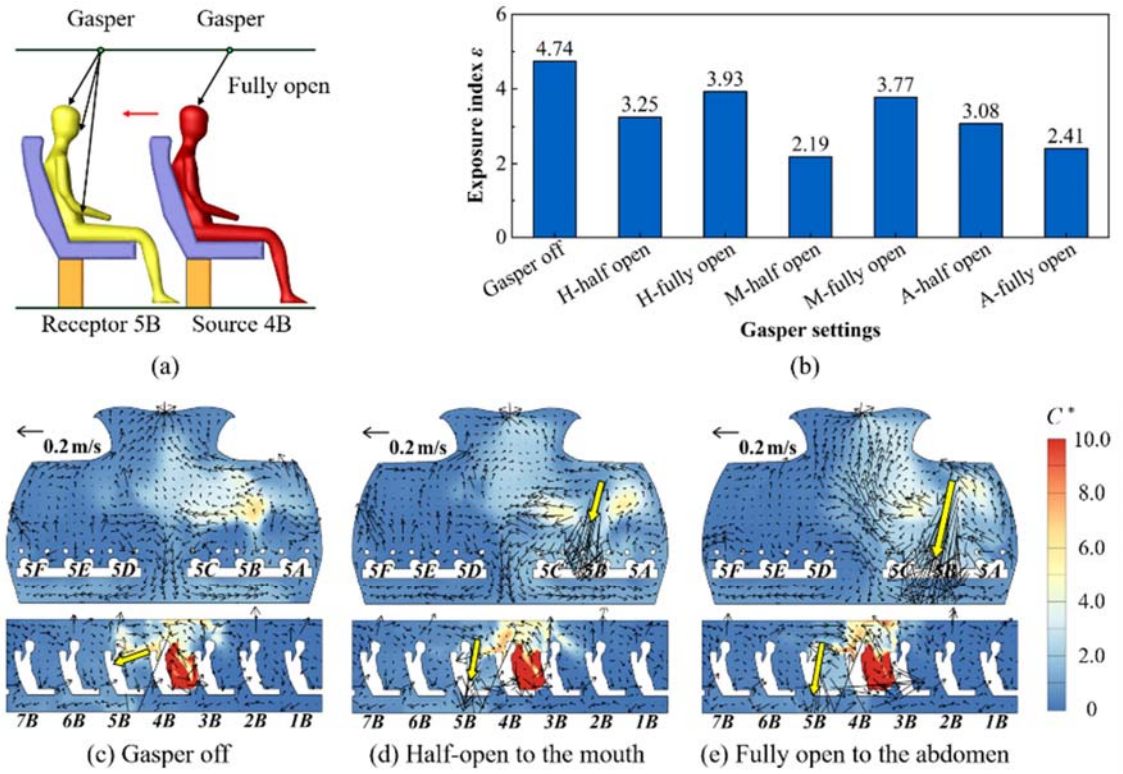

Fig. 12. (a) The relative positions of the source passenger and the receptor, (b) exposure index of the receptor 5B, and (c-e) airflow patterns and C^* distribution at CS5 and LSB under different receptor gasper settings.

5.3 Aisle seat

Among all receptors in the aisle seats, the highest exposure index was 7.98 (see Fig. A.3(c)). This most at-risk receptor was seated at 4C, with the source passenger in 4B keeping the source gasper fully open to the abdomen, as shown in Fig. 13(a). The exposure index of the receptor 4C under different gasper

settings is shown in Fig. 13(b). Turning the receptor's gasper off was used as the benchmark, with an exposure index of 7.98. The results showed that opening the receptor's gasper performed better than the benchmark. Possible reasons are as follows. When the receptor's gasper was turned off, the contaminants was transported to the receptor at thigh level by the jet flow of the source's gasper, and then carried by the thermal plume upwards into the receptor's breathing zone, as indicated by the yellow arrow in Fig. 13(c). If the receptor's gasper was open, the downward gasper jet altered the air flow pattern in front of 4C. For instance, the airflow in front of 4C was downward when the gasper was half-open to the mouth as shown in Fig. 13(d). Thus, the jet flow could effectively decrease the contaminant concentration in the receptor's breathing zone, and a stronger gasper jet performed better (see Fig. 13(e)).

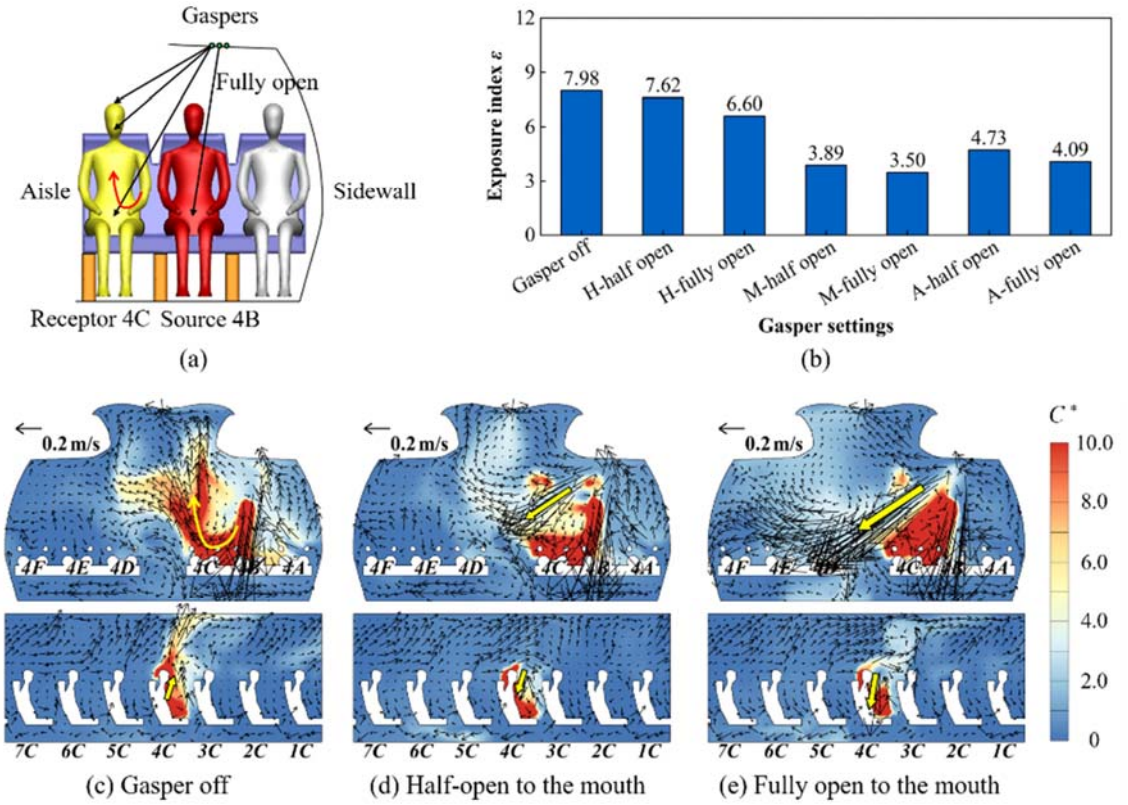

Fig. 13. (a) The relative positions of the source passenger and the receptor, (b) exposure index of the receptor 4C, and (c-e) airflow patterns and C* distribution at CS4 and LSC under different receptor gasper settings.

5.4 Protective effect and working mechanism

As illustrated in previous sections, the impact of the gasper on the three most at-risk receptors varied with different gaper settings. As summarized in Table 2, the mean exposure index was also calculated to evaluate the overall impact of turning on the receptor's gasper. When the receptor's gasper was turned on, the overall mean exposure index of three target receptors was 5.75, 21.7% lower than the benchmark

(7.34). Therefore, turning on a receptor's gasper with an appropriate setting could be an effective strategy to protect the receptor.

Table 2. Exposure index of the target receptor for different receptor's gasper settings.

Receptor	Gasper off	Gasper on					
		Head half-open	Head fully open	Mouth half-open	Mouth fully open	Abdomen half-open	Abdomen fully open
4A	9.29	25.40	2.74	11.51	3.38	3.19	8.28
5B	4.74	3.25	3.93	2.19	3.77	3.08	2.41
4C	7.98	7.62	6.60	3.89	3.50	4.73	4.09
Overall Mean	7.34	5.75					

Based on the analysis of the impact of the gasper on the three most at-risk receptors, the working mechanism of a receptor's gasper can be described as follows:

- The gasper-induced jet flow entrained the surrounding air to the jet region, leading to either a positive or negative impact on the receptor's exposure. Since the gaspers were mounted on the ceiling, if the contaminant concentration at ceiling level was low, the gasper flow entrained clean air to the lower part of the cabin and thus reduced the concentration in the receptor's breathing zone. If the concentration at ceiling level was high, directing the gasper with a low flow rate to the mouth or head resulted in a high contaminant concentration in the receptor's breathing zone.
- With a suitable gasper direction and flow rate, the gasper jet formed a virtual barrier between the source passenger and the receptor. This mechanism reduced the contaminant transmission to the receptor's breathing zone.
- When the contaminants were transported upwards to the receptor's breathing zone, turning on the receptor's gasper reduced the contaminant concentration, since the downward gasper jet altered the airflow pattern in front of the receptor.

6. Discussion

To evaluate whether the selected cases in Section 5 were representative, we analysed the transmission route of the contaminants for each receptor from the calculations in Section 4 (see Fig. A.10-13). For the first typical scenario, the contaminants entered the receptor's breathing zone either from ceiling level or horizontally at breathing level. We designated this scenario as the ceiling/breathing (C/B) scenario. For the other typical scenario, the contaminants were transported upwards to the receptor's breathing zone from floor level or from thigh level due to the thermal plume before entering the receptor's breathing zone. This scenario was designated as the floor/thigh (F/T) scenario. The calculated

probability of each scenario and the exposure range of receptors for each seat type are shown in Fig. 14. When the gasper of the source passenger was off, as depicted in Fig. 14(a), the C/B scenario had a higher probability of occurrence. Moreover, as shown in Fig. 14(b), receptors under the C/B scenario had higher mean and peak exposure values. Therefore, the C/B scenario was the most common and dangerous scenario when the source gasper was turned off. For the receptor in the window seat in Section 5.1, the source gasper was off and the contaminants were transported at breathing level into the receptor's breathing zone. Thus, it was a representative case. When the source gasper was open, as depicted in Fig. 14(c) and (d), the C/B scenario also had a higher probability of occurrence, but with a lower mean exposure index compared with the F/T scenario. Therefore, both the C/B and F/T scenarios were typical. For the receptor in the middle seat in Section 5.2 and the receptor in the aisle seat in Section 5.3, the source gasper was open and the contaminants were transported from breathing level and thigh level, respectively. Therefore, all three of the selected cases in Section 5 represent typical scenarios.

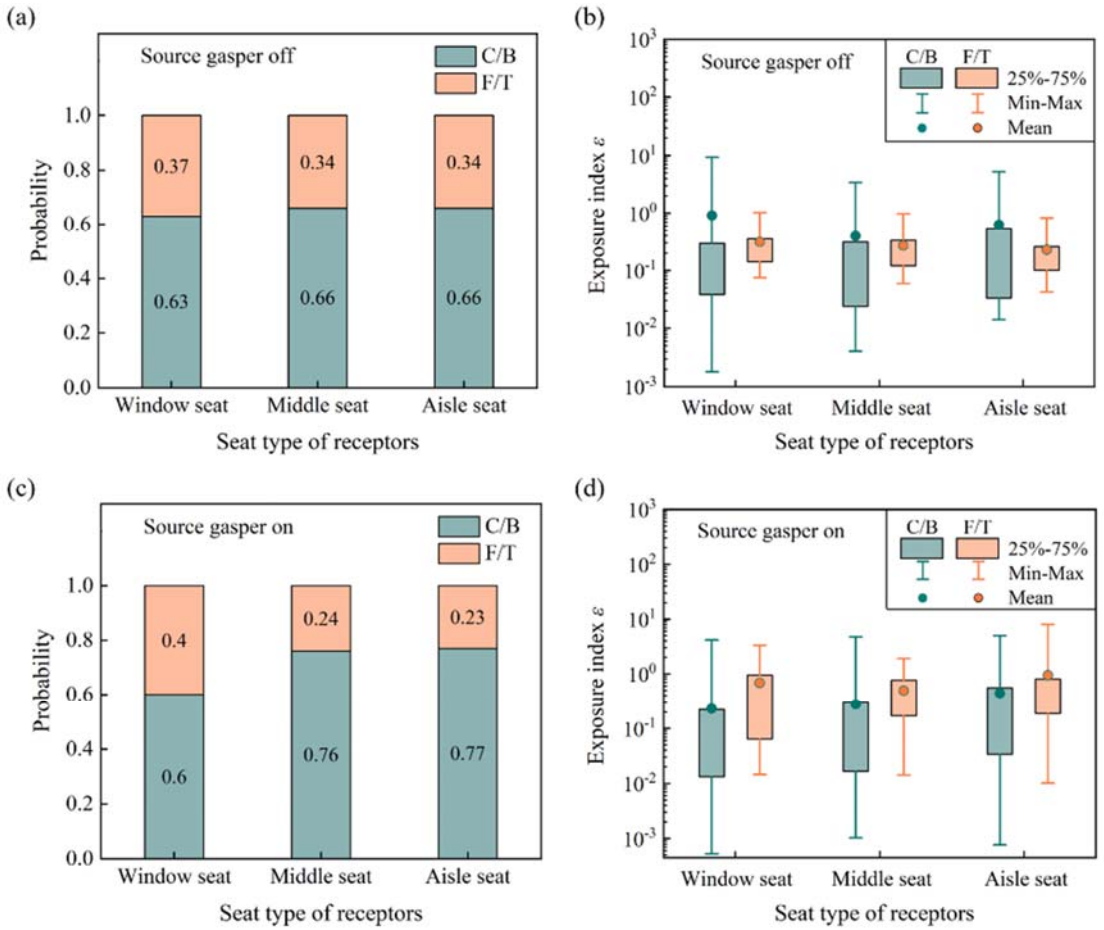

Fig. 14. When the source gasper was turned off, (a) the probability and (b) exposure of receptors for different scenarios and receptor seat types; and when the source gasper was turned on, (c) the probability and (d) exposure of receptors for different scenarios and receptor seat types.

Fig. 15 shows the airflow pattern at the window seat in longitudinal section LSA. In the middle section, the airflow under the seat was backward, while it was forward in the front and rear sections. This is because of the cabin's partitions at the front and the back of the cabin. The difference in airflow structure would further affect the contaminant transmission. In this study we only investigated the seven rows in the middle of the cabin. For the front or rear section of the cabin, the results and conclusions may be different. Further studies are needed to examine the effects of longitudinal flow and extend our findings to the whole cabin.

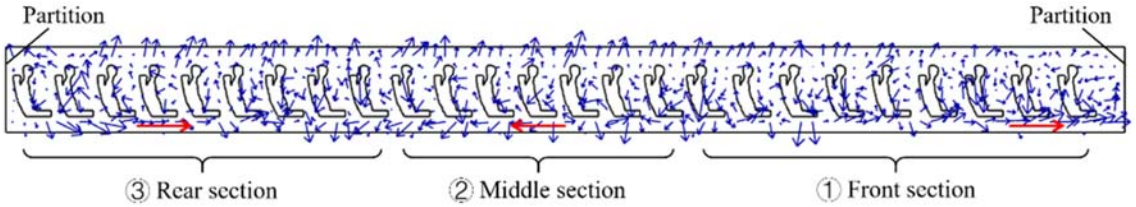

Fig. 15. The airflow pattern at LSA in a 25-row, single-aisle, fully occupied, economy-class aircraft cabin.

This study only considered three most at-risk receptors, and the gaspers of other passengers were assumed to be closed. Note that each passenger may choose whether to turn on his/her gasper. Other possible gasper on/off distributions were not addressed in this study, and current results were not sufficient to provide recommendations for gasper settings. Moreover, as mixing ventilation is prevalently used in commercial airliners, it is worthwhile to compare the performance of gaspers in different ventilation systems. Therefore, follow-up studies are needed for practical applications in the future.

7. Conclusions

This study aimed to investigate the impact of gaspers on airborne disease transmission in an aircraft cabin with a personalized displacement ventilation system. We conducted numerical studies in a seven-row section of a single-aisle, fully occupied, economy-class aircraft cabin with the CFD simulation method. We first investigated the impact of source gasper direction and flow rate on the airborne transmission near the source. Next, we investigated the protective effect of the receptor's gasper. Within the scope of this study, the following conclusions can be made:

- For a source passenger's gasper, the direction and flow rate of the gasper flow either increased or decreased the air contaminant transmission to other passengers. Directing the source gasper to the abdomen with a medium flow rate significantly mitigated the overall exposure, as this approach minimized the contaminant circulation in the aircraft cabin. This setting was recommended for the source passenger, and could reduce the mean exposure index by at least 45% compared to the benchmark.

- For a receptor's gasper, turning on the gasper with an appropriate setting could be an effective strategy to protect the receptor. The working mechanism of a receptor's gasper can be summarized as follows:

  (1) The gasper-induced jet flow entrained the surrounding air into the jet region, leading to either a positive or negative impact on the receptor's exposure. The protective effect depended on the contaminant concentration at ceiling level.

  (2) With a suitable gasper direction and flow rate, the gasper jet formed a virtual barrier between the source passenger and the receptor. This mechanism reduced the contaminant transmission to the receptor's breathing zone.

  (3) When the contaminants were transported upwards to the receptor's breathing zone, turning on the receptor's gasper reduced the contaminant concentration, since the downward gasper jet altered the airflow pattern in front of the receptor.

CRediT authorship contribution statement

Yunge Hou: Writing – original draft, Methodology, Investigation. **Ruoyu You**: Writing – review & editing, Supervision, Funding acquisition, Conceptualization.

Declaration of competing interest

The authors declare that they have no known competing financial interests or personal relationships that could have appeared to influence the work reported in this paper.

Acknowledgements

This work was supported by the Early Career Scheme (Grant No. 25210419) of Research Grants Council of Hong Kong SAR, China.

Appendix

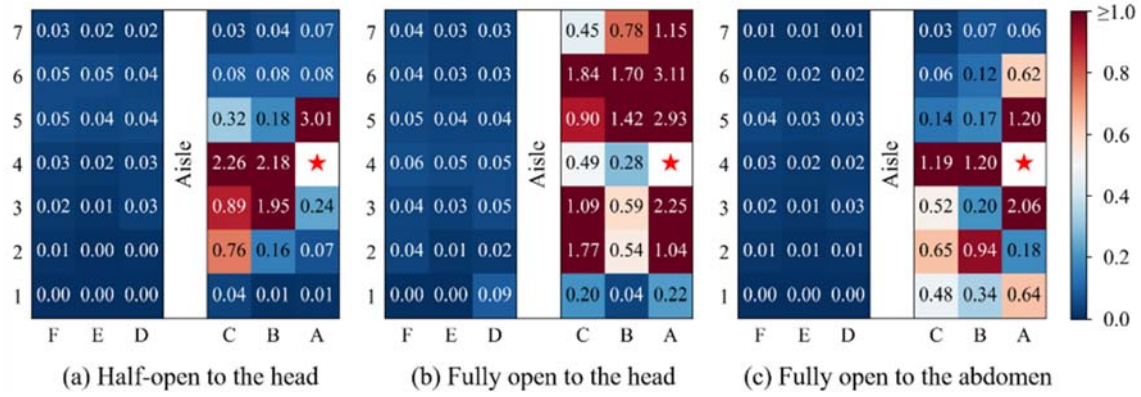

Fig. A.1. Exposure index under different gasper settings with the source passenger seated in the window seat 4A.

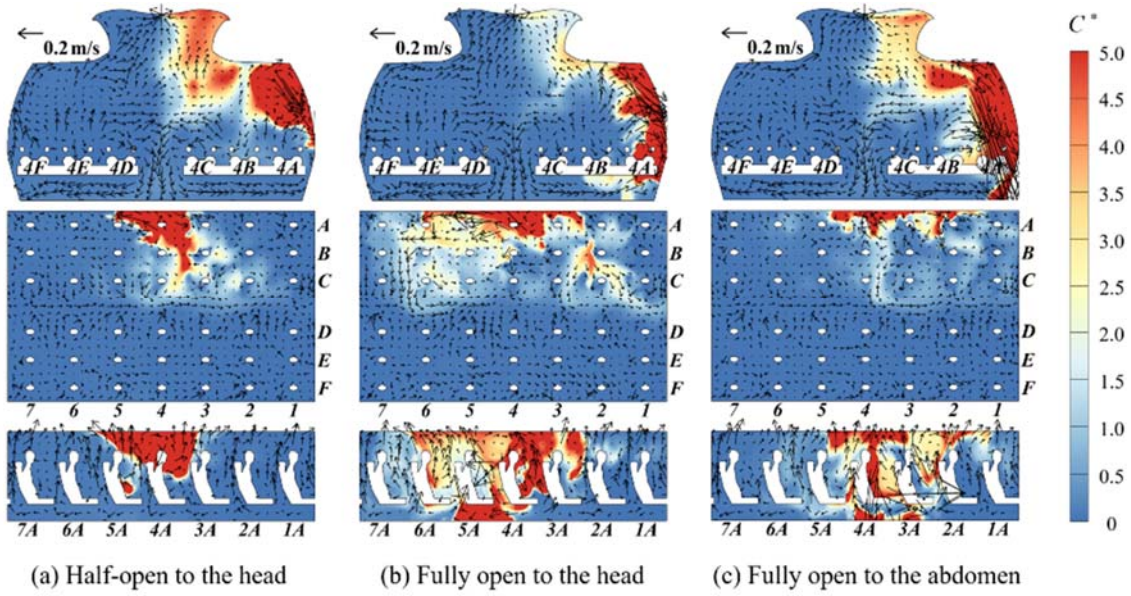

Fig. A.2. The airflow patterns and C^* distributions at CS4, HS, and LSA under different gasper settings with the source passenger seated in the window seat 4A.

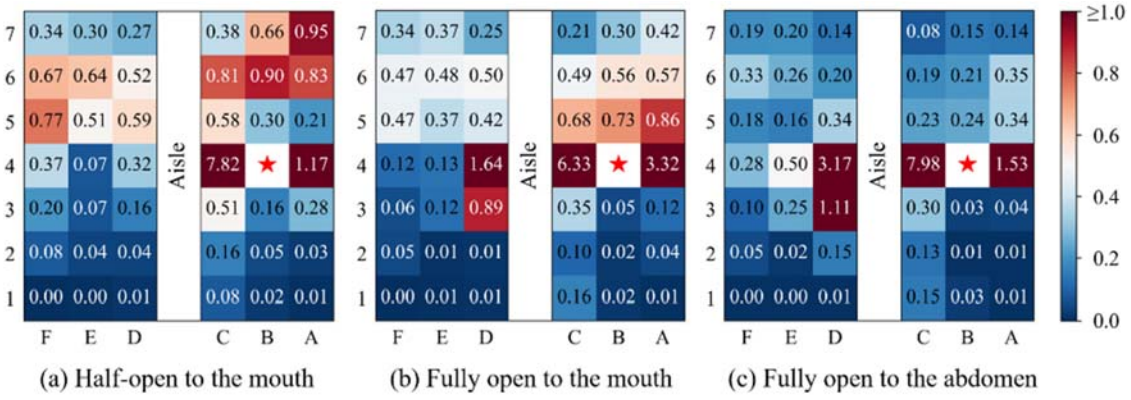

Fig. A.3. Exposure index under different gasper settings with the source passenger seated in the middle seat 4B.

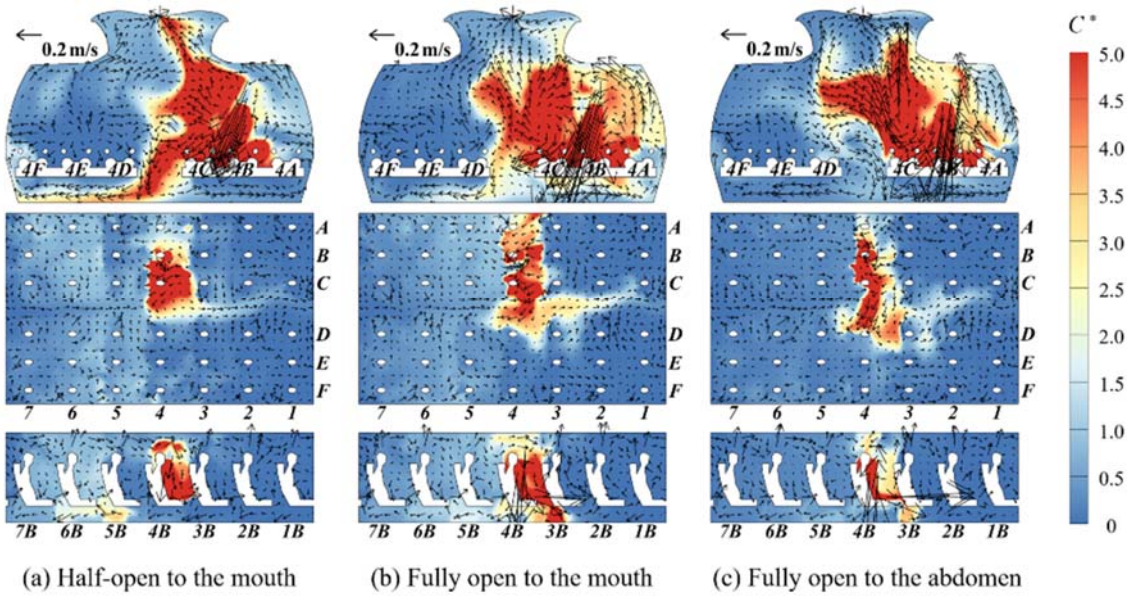

Fig. A.4. The airflow patterns and C^* distributions at CS4, HS, and LSB under different gasper settings with the source passenger seated in the middle seat 4B.

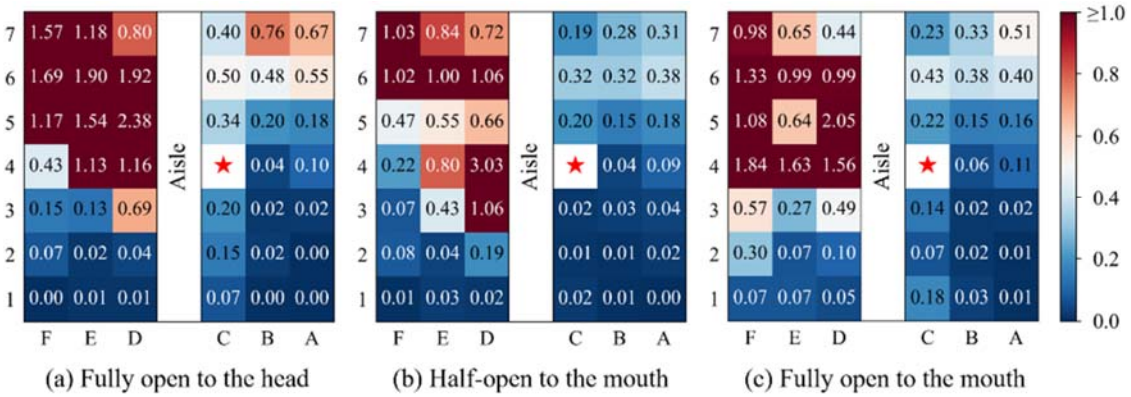

Fig. A.5. Exposure index under different gasper settings with the source passenger seated in the aisle seat 4C.

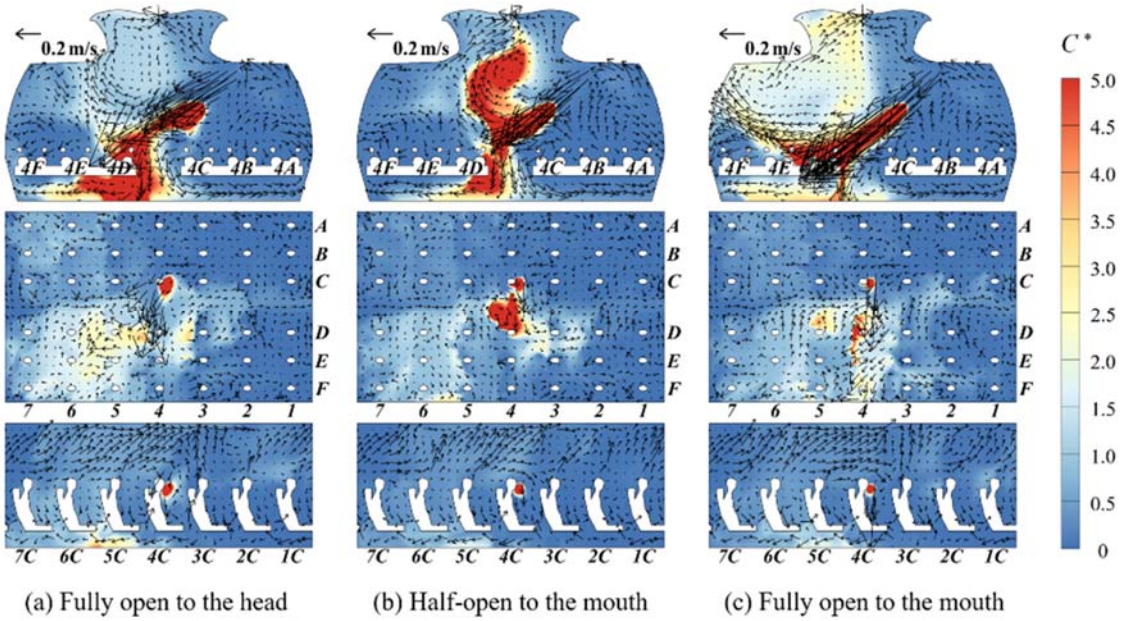

Fig. A.6. The airflow patterns and C^* distributions at CS4, HS, and LSC under different gasper settings with the source passenger seated in the aisle seat 4C.

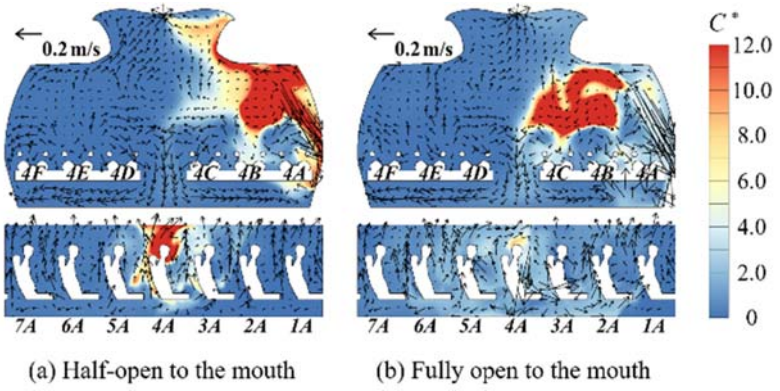

Fig. A.7. The airflow patterns and C^* distributions at CS4 and LSA under different gasper settings with the receptor seated in the window seat 4A.

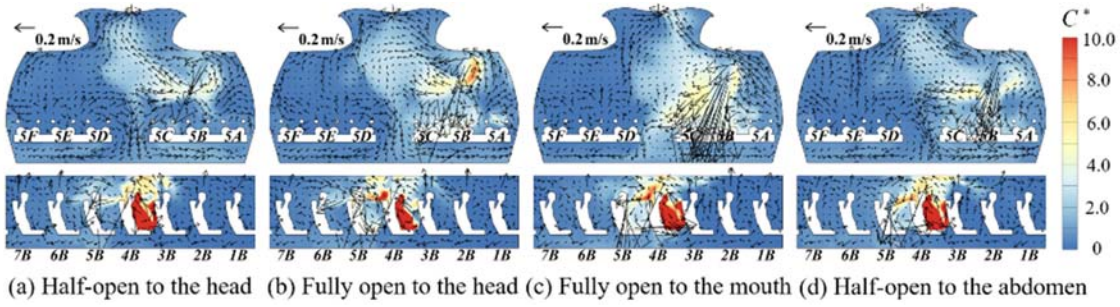

Fig. A.8. The airflow patterns and C^* distributions at CS5 and LSB under different gasper settings with the receptor seated in the middle seat 5B.

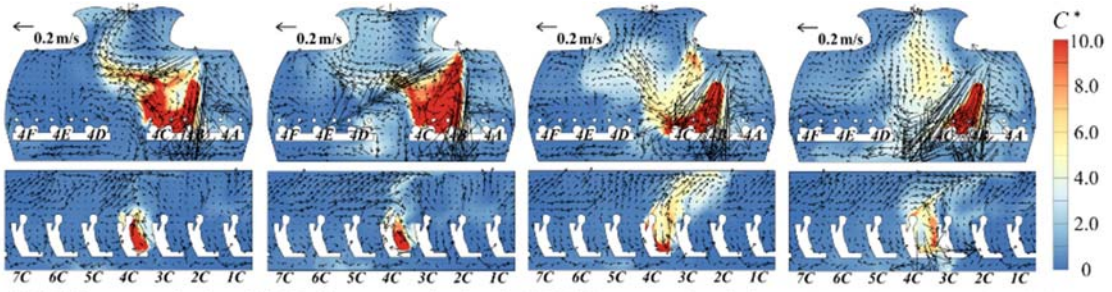

(a) Half-open to the head (b) Fully open to the head (c) Half-open to the abdomen (d) Fully open to the abdomen

Fig. A.9. The airflow patterns and C^* distributions at CS4 and LSC under different gasper settings with the receptor seated in the aisle seat 4C.

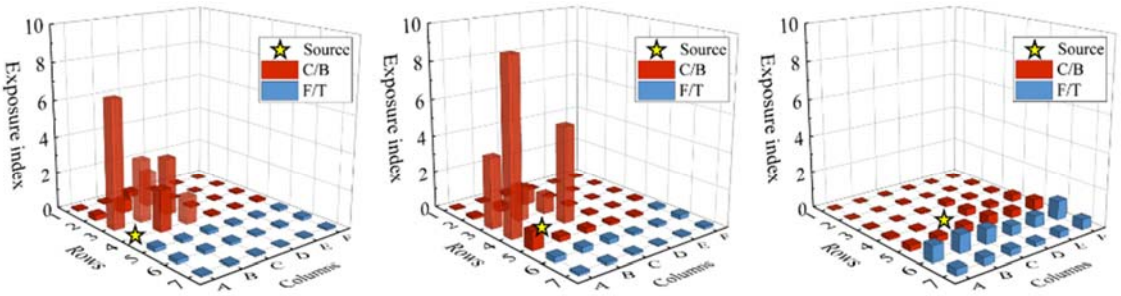

(a) Source 4A with gasper off (b) Source 4B with gasper off (c) Source 4C with gasper off

Fig. A.10. Distribution of scenarios for all receptors when the gasper of the source passenger was off.

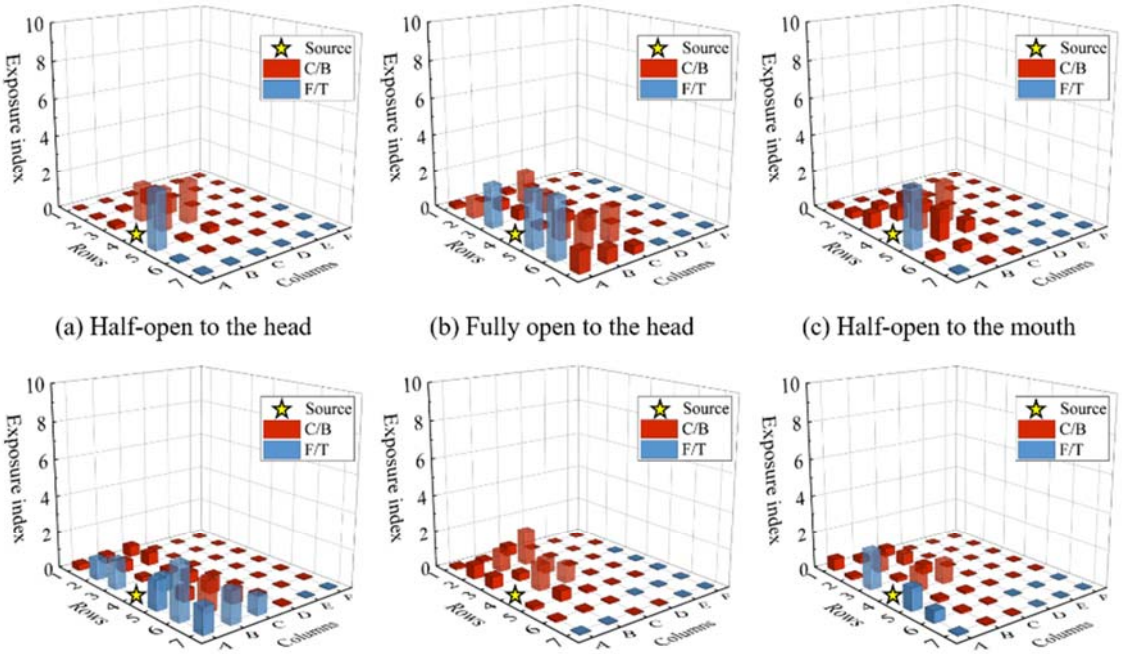

(a) Half-open to the head (b) Fully open to the head (c) Half-open to the mouth

(d) Fully open to the mouth (e) Half-open to the abdomen (f) Fully open to the abdomen

Fig. A.11. Distribution of scenarios for all receptors when the gasper of the source passenger 4A was on.

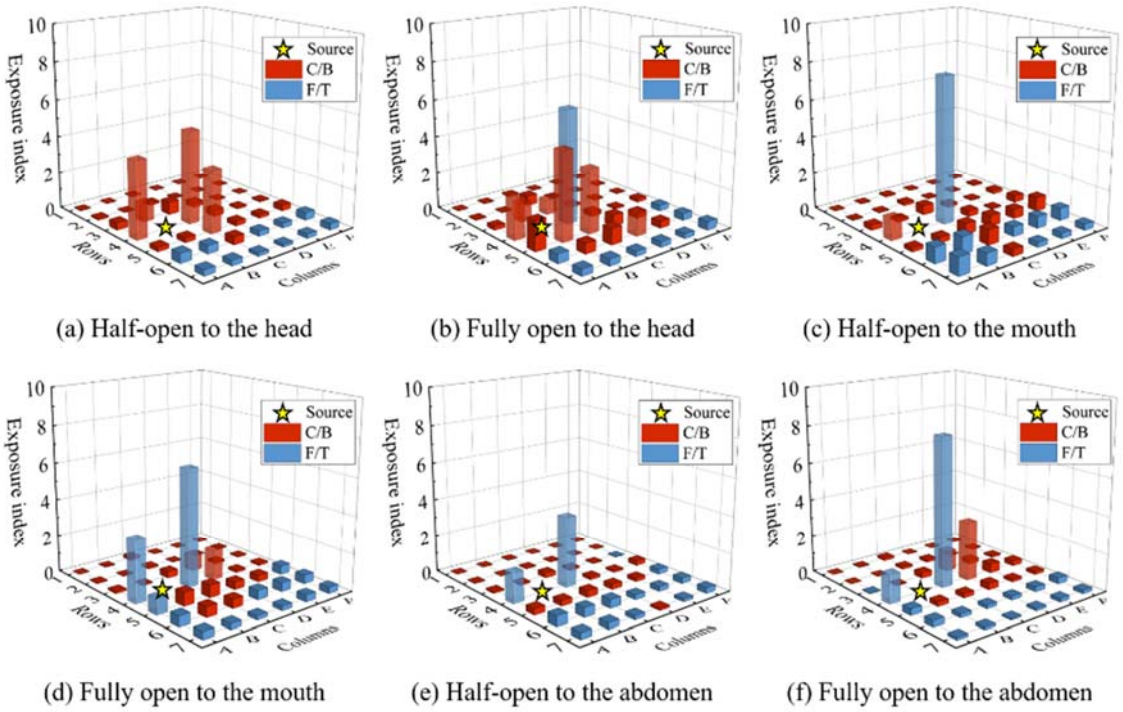

Fig. A.12. Distribution of scenarios for all receptors when the gasper of the source passenger 4B was on.

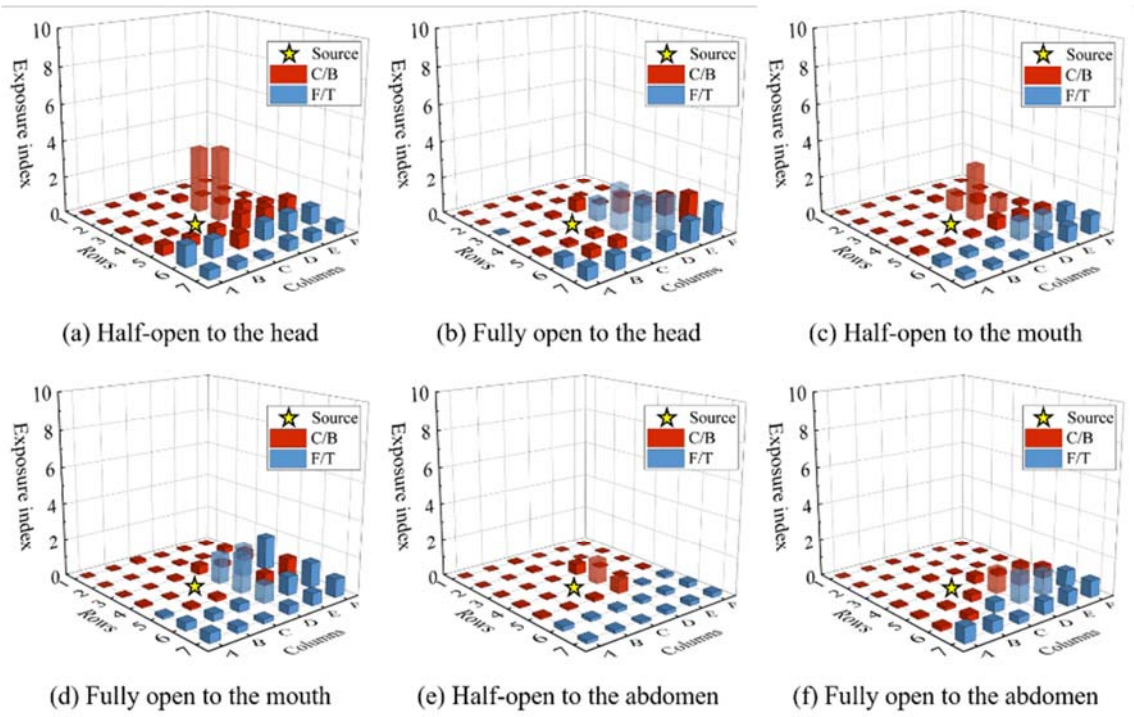

Fig. A.13. Distribution of scenarios for all receptors when the gasper of the source passenger 4C was on.

References

[1] IATA, Number of scheduled passengers boarded by the global airline industry from 2004 to 2022. https://www.statista.com/statistics/564717/airline-industry-passenger-traffic-globally/, (accessed 28 May 2023).

[2] M.R. Moser, T.R. Bender, H.S. Margolis, G.R. Noble, A.P. Kendal, D.G. Ritter, An outbreak of influenza aboard a commercial airliner, Am. J. Epidemiol. 110(1) (1979) 1-6. https://doi.org/10.1093/oxfordjournals.aje.a112781.

[3] S.J. Olsen, H.-L. Chang, T.Y.-Y. Cheung, A.F.-Y. Tang, T.L. Fisk, S.P.-L. Ooi, H.-W. Kuo, D.D.-S. Jiang, K.-T. Chen, J. Lando, Transmission of the severe acute respiratory syndrome on aircraft, N. Engl. J. Med. 349(25) (2003) 2416-2422. https://doi.org/10.1056/NEJMoa031349.

[4] A. Mangili, M.A. Gendreau, Transmission of infectious diseases during commercial air travel, Lancet 365(9463) (2005) 989-996. https://doi.org/10.1016/S0140-6736(05)71089-8.

[5] J.K. Gupta, C.H. Lin, Q. Chen, Risk assessment of airborne infectious diseases in aircraft cabins, Indoor air 22(5) (2012) 388-395. https://doi.org/10.1111/j.1600-0668.2012.00773.x.

[6] N.C. Khanh, P.Q. Thai, H.-L. Quach, N.-A.H. Thi, P.C. Dinh, T.N. Duong, N.D. Nghia, T.A. Tu, T. Dai Quang, T.-T. Nguyen, Transmission of SARS-CoV 2 during long-haul flight, Emerg. Infect. Dis. 26(11) (2020) 2617-2624. https://doi.org/10.3201/eid2611.203299.

[7] Y. Li, G.M. Leung, J. Tang, X. Yang, C. Chao, J.Z. Lin, J. Lu, P.V. Nielsen, J. Niu, H. Qian, Role of ventilation in airborne transmission of infectious agents in the built environment-a multidisciplinary systematic review, Indoor air 17(1) (2007) 2-18. https://doi.org/10.1111/j.1600-0668.2006.00445.x.

[8] N. Gao, J. Niu, Personalized ventilation for commercial aircraft cabins, J. Aircraft 45(2) (2008) 508-512. https://doi.org/10.2514/1.30272.

[9] J. Fišer, M. Jícha, Impact of air distribution system on quality of ventilation in small aircraft cabin, Build. Environ. 69 (2013) 171-182. https://doi.org/10.1016/j.buildenv.2013.08.007.

[10] F. Wang, R. You, T. Zhang, Q. Chen, Recent progress on studies of airborne infectious disease transmission, air quality, and thermal comfort in the airliner cabin air environment, Indoor air 32(4) (2022) e13032. https://doi.org/10.1111/ina.13032.

[11] Z. Zhang, X. Chen, S. Mazumdar, T. Zhang, Q. Chen, Experimental and numerical investigation of airflow and contaminant transport in an airliner cabin mockup, Build. Environ. 44(1) (2009) 85-94. https://doi.org/10.1016/j.buildenv.2008.01.012.

[12] Y. Zhang, J. Liu, J. Pei, J. Li, C. Wang, Performance evaluation of different air distribution systems in an aircraft cabin mockup, Aero. Sci. Technol. 70 (2017) 359-366. https://doi.org/10.1016/j.ast.2017.08.009.

[13] R. You, C.H. Lin, D. Wei, Q. Chen, Evaluating the commercial airliner cabin environment with different air distribution systems, Indoor Air 29(5) (2019) 840-853. https://doi.org/10.1111/ina.12578.

[14] M. Liu, J. Liu, Q. Cao, X. Li, S. Liu, S. Ji, C.-H. Lin, D. Wei, X. Shen, Z. Long, Evaluation of different air distribution systems in a commercial airliner cabin in terms of comfort and COVID-19 infection risk, Build. Environ. 208 (2022) 108590. https://doi.org/10.1016/j.buildenv.2021.108590.

[15] M. Liu, D. Chang, J. Liu, S. Ji, C.-H. Lin, D. Wei, Z. Long, T. Zhang, X. Shen, Q. Cao, Experimental investigation of air distribution in an airliner cabin mockup with displacement ventilation, Build. Environ. 191 (2021) 107577. https://doi.org/10.1016/j.buildenv.2020.107577.

[16] T. Zhang, Q.Y. Chen, Novel air distribution systems for commercial aircraft cabins, Build. Environ. 42(4) (2007) 1675-1684. https://doi.org/10.1016/j.buildenv.2006.02.014.

[17] P. Zítek, T. Vyhlídal, G. Simeunović, L. Nováková, J. Čížek, Novel personalized and humidified air supply for airliner passengers, Build. Environ. 45(11) (2010) 2345-2353. https://doi.org/10.1016/j.buildenv.2010.04.005.

[18] T.T. Zhang, P. Li, S. Wang, A personal air distribution system with air terminals embedded in chair armrests on commercial airplanes, Build. Environ. 47 (2012) 89-99. https://doi.org/10.1016/j.buildenv.2011.04.035.

[19] R. You, Y. Zhang, X. Zhao, C.-H. Lin, D. Wei, J. Liu, Q. Chen, An innovative personalized displacement ventilation system for airliner cabins, Build. Environ. 137 (2018) 41-50. https://doi.org/10.1016/j.buildenv.2018.03.057.

[20] S. Dai, H. Sun, W. Liu, Y. Guo, N. Jiang, J. Liu, Experimental study on characteristics of the jet flow from an aircraft gasper, Build. Environ. 93 (2015) 278-284. https://doi.org/10.1016/j.buildenv.2015.06.006.

[21] Z. Shi, J. Chen, R. You, C. Chen, Q. Chen, Modeling of gasper-induced jet flow and its impact on cabin air quality, Energy Build. 127 (2016) 700-713. https://doi.org/10.1016/j.enbuild.2016.06.038.

[22] J. Li, J. Liu, S. Dai, Y. Guo, N. Jiang, W. Yang, PIV experimental research on gasper jets interacting with the main ventilation in an aircraft cabin, Build. Environ. 138 (2018) 149-159. https://doi.org/10.1016/j.buildenv.2018.04.023.

[23] B. Li, R. Duan, J. Li, Y. Huang, H. Yin, C.H. Lin, D. Wei, X. Shen, J. Liu, Q. Chen, Experimental studies of thermal environment and contaminant transport in a commercial aircraft cabin with gaspers on, Indoor air 26(5) (2016) 806-819. https://doi.org/10.1111/ina.12265.

[24] R. You, J. Chen, Z. Shi, W. Liu, C.-H. Lin, D. Wei, Q. Chen, Experimental and numerical study of airflow distribution in an aircraft cabin mock-up with a gasper on, J. Build. Perform. Simulat. 9(5) (2016) 555-566. https://doi.org/10.1080/19401493.2015.1126762.

[25] R. You, W. Liu, J. Chen, C.-H. Lin, D. Wei, Q. Chen, Predicting airflow distribution and contaminant transport in aircraft cabins with a simplified gasper model, J. Build. Perform. Simulat. 9(6) (2016) 699-708. https://doi.org/10.1080/19401493.2016.1196730.

[26] R. You, J. Chen, C.-H. Lin, D. Wei, Q. Chen, Investigating the impact of gaspers on cabin air quality in commercial airliners with a hybrid turbulence model, Build. Environ. 111 (2017) 110-122. https://doi.org/10.1016/j.buildenv.2016.10.018.

[27] Z. Fang, H. Liu, B. Li, A. Baldwin, J. Wang, K. Xia, Experimental investigation of personal air supply nozzle use in aircraft cabins, Appl. Ergon. 47 (2015) 193-202. https://doi.org/10.1016/j.apergo.2014.09.011.

[28] W. Cui, T. Wu, Q. Ouyang, Y. Zhu, Passenger thermal comfort and behavior: a field investigation in commercial aircraft cabins, Indoor air 27(1) (2017) 94-103. https://doi.org/10.1111/ina.12294.

[29] A. ASHRAE, Standard 161–2018, Air Quality within Commercial Aircraft, American Society of Heating, Refrigerating and Air-Conditioning Engineers, Inc, Atlanta, 2018.

[30] W. Liu, S. Mazumdar, Z. Zhang, S.B. Poussou, J. Liu, C.-H. Lin, Q. Chen, State-of-the-art methods for studying air distributions in commercial airliner cabins, Build. Environ. 47 (2012) 5-12. https://doi.org/10.1016/j.buildenv.2011.07.005.

[31] Z. Shi, J. Chen, Q. Chen, On the turbulence models and turbulent Schmidt number in simulating stratified flows, J. Build. Perform. Simulat. 9(2) (2016) 134-148. https://doi.org/10.1080/19401493.2015.1004109.

[32] A. Fluent, Ansys fluent Theory Guide, Release, Canonsburg, USA (2022), 2023 R1.

[33] F.R. Menter, Two-equation eddy-viscosity turbulence models for engineering applications, AIAA J. 32(8) (1994) 1598-1605. https://doi.org/10.2514/3.12149.

[34] Z. Zhang, Q. Chen, Comparison of the Eulerian and Lagrangian methods for predicting particle transport in enclosed spaces, Atmos. Environ. 41(25) (2007) 5236-5248. https://doi.org/10.1016/j.atmosenv.2006.05.086.

[35] Y. Lu, M. Oladokun, Z. Lin, Reducing the exposure risk in hospital wards by applying stratum ventilation system, Build. Environ. 183 (2020) 107204. https://doi.org/10.1016/j.buildenv.2020.107204.

[36] C.K. Ho, Modeling airborne pathogen transport and transmission risks of SARS-CoV-2, Appl. Math. Model. 95 (2021) 297-319. https://doi.org/10.1016/j.apm.2021.02.018.

[37] S. Srivastava, X. Zhao, A. Manay, Q. Chen, Effective ventilation and air disinfection system for reducing coronavirus disease 2019 (COVID-19) infection risk in office buildings, Sustain. Cities Soc. 75 (2021) 103408. https://doi.org/10.1016/j.scs.2021.103408.

[38] X. Zhao, S. Liu, Y. Yin, T. Zhang, Q. Chen, Airborne transmission of COVID‐19 virus in enclosed spaces: an overview of research methods, Indoor air 32(6) (2022) e13056. https://doi.org/10.1111/ina.13056.

[39] D.D. Gray, A. Giorgini, The validity of the Boussinesq approximation for liquids and gases, Int. J. Heat Mass Tran. 19(5) (1976) 545-551. https://doi.org/10.1016/0017-9310(76)90168-X.

[40] S.V. Patankar, Numerical heat transfer and fluid flow, Hemisphere Publ, New York, 1980.

[41] SeatGuru. https://www.seatguru.com/findseatmap/findseatmap.php/, (accessed 4 March 2023).

[42] H. Qian, Y. Li, Removal of exhaled particles by ventilation and deposition in a multibed airborne infection isolation room, Indoor air 20(4) (2010) 284-297. https://doi.org/10.1111/j.1600-0668.2010.00653.x.

[43] I. Olmedo, P.V. Nielsen, M. Ruiz de Adana, R.L. Jensen, P. Grzelecki, Distribution of exhaled contaminants and personal exposure in a room using three different air distribution strategies, Indoor air 22(1) (2012) 64-76. https://doi.org/10.1111/j.1600-0668.2011.00736.x.

[44] L. Liu, Y. Li, P.V. Nielsen, J. Wei, R.L. Jensen, Short‐range airborne transmission of expiratory droplets between two people, Indoor air 27(2) (2017) 452-462. https://doi.org/10.1111/ina.12314.

[45] Z. Ai, T. Huang, A. Melikov, Airborne transmission of exhaled droplet nuclei between occupants in a room with horizontal air distribution, Build. Environ. 163 (2019) 106328. https://doi.org/10.1016/j.buildenv.2019.106328.

[46] United States Department of Labour, OSHA Technical Manual (OTM) - Section II: Chapter 1 | Occupational Safety and Health Administration. https://www.osha.gov/otm/section-2-health-hazards/chapter-1, (accessed 24 March 2023)

[47] D. Frank, P. Linden, The effectiveness of an air curtain in the doorway of a ventilated building, J. Fluid Mech. 756 (2014) 130-164. https://doi.org/10.1017/jfm.2014.433.